GRAVITATIONAL WAVES[*][†]

Kip S. Thorne
Theoretical Astrophysics, California Institute of Technology
Pasadena, California 91125

ABSTRACT

These lectures review current efforts and plans for gravitational-wave detection, the gravitational-wave sources that might be detected, and the information that the detectors might extract from the observed waves. Special attention is paid to (1) the LIGO/VIRGO network of earth-based, kilometer-scale laser interferometers, which is now under construction and will operate in the high-frequency band (1 to 10^4 Hz), and (2) a proposed five-million-kilometer-long Laser Interferometer Space Antenna (LISA), which would fly in heliocentric orbit and operate in the low-frequency band (10^{-4} to 1 Hz). LISA would extend the LIGO/VIRGO studies of stellar-mass ($M \sim 2$ to $300\ M_\odot$) black holes into the domain of the massive black holes ($M \sim 1000$ to $10^8\ M_\odot$) that inhabit galactic nuclei and quasars.

---

[*] SUPPORTED IN PART BY NSF GRANTS AST-9417371 AND PHY-9424337, AND BY NASA GRANT NAGW-4268. THIS ARTICLE IS ALSO BEING PUBLISHED AS A CHAPTER IN THE *PROCEEDINGS OF THE SNOWMASS '94 SUMMER STUDY ON PARTICLE AND NUCLEAR ASTROPHYSICS AND COSMOLOGY*, EDITED BY E. W. KOLB AND R. PECCEI (WORLD SCIENTIFIC, SINGAPORE, 1995).

[†] THIS CONTRIBUTION COVERS IN PART THE R. WEISS PRESENTATION AT THE 1994 SLAC SUMMER INSTITUTE.

1 Introduction

According to general relativity theory, compact concentrations of energy (e.g., neutron stars and black holes) should warp spacetime strongly, and whenever such an energy concentration changes shape, it should create a dynamically changing spacetime warpage that propagates out through the universe at the speed of light. This propagating warpage is called a *gravitational wave*—a name that arises from general relativity's description of gravity as a consequence of spacetime warpage.

Although gravitational waves have not yet been detected directly, their indirect influence has been seen and measured with such remarkable accuracy that their reality has been blessed even by the Nobel Prize Committee (that bastion of conservatism which explicitly denied Einstein the Prize for his relativity theories[1]).

The 1993 Prize was awarded to Russell Hulse and Joseph Taylor for their discovery of the binary pulsar PSR 1913+16 (Ref. 2) and for Taylor's observational demonstration (with colleagues)[3] that the binary's two neutron stars are spiraling together at just the rate predicted by general relativity's theory of gravitational radiation reaction. From the observed orbit, one can compute the rate at which orbital energy should be emitted into gravitational radiation, and from this rate of energy loss, one can compute the rate of orbital inspiral. The computed and observed inspiral rates agree to within the experimental accuracy, better than 1%.

Although this is a great triumph for Einstein, it is not a firm proof that general relativity is correct in all respects. Other relativistic theories of gravity (theories compatible with special relativity) predict the existence of gravitational waves; and some other theories predict the same inspiral rate for PSR 1913+16 as general relativity, to within the experimental accuracy.[4,5] Nevertheless, the experimental evidence for general relativity is so strong[4] that I shall assume it to be correct throughout this lecture except for occasional side remarks.

There are a number of efforts, worldwide, to detect gravitational radiation. These efforts are driven in part by the desire to "see gravitational waves in the flesh," but more importantly, by the goal of using the waves as a probe of the universe and of the nature of gravity. And a powerful probe they should be, since they carry detailed information about gravity and their sources.

There is an enormous difference between gravitational waves and the electromagnetic waves on which our present knowledge of the universe is based:

- Electromagnetic waves are oscillations of the electromagnetic field that propagate through spacetime; gravitational waves are oscillations of the "fabric" of spacetime itself.
- Astronomical electromagnetic waves are almost always incoherent superpositions of emission from individual electrons, atoms, or molecules. Cosmic gravitational waves are produced by coherent, bulk motions of huge amounts of mass-energy—either material mass or the energy of vibrating, nonlinear spacetime curvature.
- Since the wavelengths of electromagnetic waves are small compared to their sources (gas clouds, stellar atmospheres, accretion disks, etc.), from the waves we can make pictures of the sources. The wavelengths of cosmic gravitational waves are comparable to or larger than their coherent, bulk-moving sources, so we cannot make pictures from them. Instead, the gravitational waves are like sound; they carry, in two independent waveforms, a stereophonic, symphony-like description of their sources.
- Electromagnetic waves are easily absorbed, scattered, and dispersed by matter. Gravitational waves travel nearly unscathed through all forms and amounts of intervening matter.[6,7]
- Astronomical electromagnetic waves have frequencies that begin at $f \sim 10^7$Hz and extend on *upward* by roughly 20 orders of magnitude. Astronomical gravitational waves should begin at $\sim 10^4$ Hz (1000-fold lower than the lowest-frequency astronomical electromagnetic waves) and should extend on *downward* from there by roughly 20 orders of magnitude.

These enormous differences make it likely that:

- The information brought to us by gravitational waves will be very different from (almost "orthogonal to") that carried by electromagnetic waves; gravitational waves will show us details of the bulk motion of dense concentrations of energy, whereas electromagnetic waves show us the thermodynamic state of optically thin concentrations of matter.
- Most (but not all) gravitational-wave sources that our instruments detect will not be seen electromagnetically, and conversely, most objects observed

electromagnetically will never be seen gravitationally. Typical electromagnetic sources are stellar atmospheres, accretion disks, and clouds of interstellar gas—none of which emit significant gravitational waves, while typical gravitational-wave sources are the cores of supernova (which are hidden from electromagnetic view by dense layers of surrounding stellar gas), and colliding black holes (which emit no electromagnetic waves at all).

- Gravitational waves may bring us great surprises. In the past, when a radically new window has been opened onto the universe, the resulting surprises have had a profound, indeed revolutionary, impact. For example, the radio universe, as discovered in the 1940s, '50s, and '60s, turned out to be far more violent than the optical universe; radio waves brought us quasars, pulsars, and the cosmic microwave radiation, and with them, our first direct observational evidence for black holes, neutron stars, and the heat of the Big Bang.[8] It is reasonable to hope that gravitational waves will bring a similar "revolution."

In this lecture, I shall review the present status of attempts to detect gravitational radiation and plans for the future, and I shall describe some examples of information that we expect to garner from the observed waves. I shall begin, in Sec. 2, with an overview of all the frequency bands in which astrophysical gravitational waves are expected to be strong, the expected sources in each band, and the detection techniques being used in each. Then in subsequent sections, I shall focus on (1) the "high frequency band" which is populated by waves from stellar mass black holes and neutron stars, and is being probed by the ground-based instruments of laser interferometers and resonant-mass antennas (Secs. 3, 4, 5, and 6), and (2) the "low-frequency band" which is populated by waves from supermassive black holes and binary stars, and is probed by the space-based instruments of radio and optical tracking of spacecraft (Secs. 7 and 8). Finally, in Sec. 9, I shall describe the stochastic background of gravitational waves that is thought to have been produced by various processes in the early universe, and prospects for detecting it in the various frequency bands.

2 Frequency Bands, Sources, and Detection Methods

Four gravitational-wave frequency bands are being explored experimentally: the high-frequency band (HF; $f \sim 10^4$ to 1 Hz), the low-frequency band (LF; $f \sim 1$ to 10^{-4} Hz), the very-low frequency band (VLF; $f \sim 10^{-7}$ to 10^{-9} Hz), and the extremely-low-frequency band (ELF; $f \sim 10^{-15}$ to 10^{-18} Hz).

2.1 High-Frequency Band, 1 to 10^4 Hz

A gravitational-wave source of mass M cannot be much smaller than its gravitational radius, $2\ GM/c^2$, and cannot emit strongly at periods much smaller than the light-travel time $4\ \pi GM/c^3$ around this gravitational radius. Correspondingly, the frequencies at which it emits are

$$f \lesssim \frac{1}{4\ \pi GM/c^3} \sim 10^4\ \mathrm{Hz} \frac{M_\odot}{M} \ , \tag{1}$$

where $M_\odot$ is the mass of the Sun, and G and c are Newton's gravitation constant and the speed of light. To achieve a size of the same order as its gravitational radius and thereby emit near this maximum frequency, an object presumably must be heavier than the Chandrasekhar limit, about the mass of the sun, $M_\odot$. Thus, the highest frequency expected for strong gravitational waves is $f_{\max} \sim 10^4$ Hz. This defines the upper edge of the high-frequency gravitational-wave band.

The high-frequency band is the domain of the Earth-based gravitational-wave detectors of laser interferometers and resonant mass antennas. At frequencies below about 1 Hz, Earth-based detectors face nearly insurmountable noise (1) from fluctuating Newtonian gravity gradients (due, e.g., to the gravitational pulls of inhomogeneities in the Earth's atmosphere which move overhead with the wind), and (2) from Earth vibrations (which are extremely difficult to filter out mechanically below ~ 1 Hz). This defines the 1 Hz lower edge of the high-frequency band; to detect waves below this frequency, one must fly one's detectors in space.

A number of interesting gravitational-wave sources fall in the high-frequency band: the stellar collapse to a neutron star or black hole in our galaxy and distant galaxies, which sometimes triggers supernova; the rotation and vibration of neutron stars (pulsars) in our galaxy; the coalescence of neutron-star and stellar-mass black-hole binaries ($M \lesssim 1000\ M_\odot$) in distant galaxies; and possibly such sources of stochastic background as vibrating loops of cosmic string, phase transitions in the early universe, and the Big Bang in which the universe was born.

I shall discuss the high-frequency band in detail in Secs. 3–6.

2.2 Low-Frequency Band, 10^{-4} to 1 Hz

The low-frequency band, 10^{-4} to 1 Hz, is the domain of detectors flown in space (in Earth orbit or in interplanetary orbit). The most important of these are the Doppler tracking of spacecraft via microwave signals sent from Earth to the spacecraft and there transponded back to Earth (a technique that NASA has pursued since the early 1970s), and optical tracking of spacecraft by each other (laser interferometry in space, a technique now under development for possible flight in ~ 2014 or sooner).

The 1 Hz upper edge of the low-frequency band is defined by the gravity-gradient and seismic cutoffs on Earth-based instruments; the $\sim 10^{-4}$ Hz lower edge is defined by expected severe difficulties at lower frequencies in isolating spacecraft from the buffeting forces of fluctuating solar radiation pressure, solar wind, and cosmic rays.

The low-frequency band should be populated by waves from short-period binary stars in our own galaxy (main-sequence binaries, cataclysmic variables, white-dwarf binaries, neutron-star binaries, etc.); from white dwarfs, neutron stars, and small black holes spiraling into massive black holes ($M \sim 3 \times 10^5$ to $3 \times 10^7\ M_\odot$) in distant galaxies; and from the inspiral and coalescence of supermassive black-hole binaries ($M \sim 100$ to $10^8\ M_\odot$). The upper limit, $\sim 10^8\ M_\odot$, on the masses of black holes that can emit in the low-frequency band is set by Eq. (1) with $f \gtrsim 10^{-4}$ Hz. There should also be a low-frequency stochastic background from such early-universe processes as vibrating cosmic strings, phase transitions, and the Big Bang itself.

I shall discuss the low-frequency band in detail in Secs. 7 and 8.

2.3 Very-Low-Frequency Band, 10^{-7} to 10^{-9} Hz

Joseph Taylor and others have achieved a remarkable gravity-wave sensitivity in the very-low-frequency band (VLF) by the timing of millisecond pulsars. When a gravitational wave passes over the Earth, it perturbs our rate of flow of time and thence the ticking rates of our clocks relative to clocks outside the wave. Such perturbations will show up as apparent fluctuations in the times of arrival of the pulsar's pulses. If no fluctuations are seen at some level, we can be rather sure that neither Earth nor the pulsar is being bathed by gravitational waves of the corresponding strength. If fluctuations with the same time evolution are seen simultaneously in the timing of several different pulsars, then the cause could well be gravitational waves bathing the Earth.

By averaging the pulses' times of arrival over long periods of time (months to tens of years), a very high timing precision can be achieved, and correspondingly, tight limits can be placed on the waves bathing the Earth or the pulsar. The upper edge of the VLF band, $\sim 10^{-7}$ Hz, is set by the averaging time of a few months needed to build up high accuracy; the lower edge, $\sim 10^{-9}$ Hz, is set by the time of ~ 20 years, since very steady millisecond pulsars were first discovered.

As we shall see in Sec. 3.2, strong gravitational-wave sources are generally compact, not much larger than their own gravitational radii. The only compact bodies that can radiate in the VLF band or below, i.e., at $f \lesssim 10^{-7}$ Hz, are those with $M \gtrsim 10^{11}\ M_\odot$ [cf. Eq. (1)]. Conventional astronomical wisdom suggests that compact bodies this massive do not exist, and that therefore, the only strong waves in the VLF band and below are a stochastic background produced by the same early-universe processes as might radiate at low and high frequencies: cosmic strings, phase transitions, and the Big Bang.

Of course, conventional wisdom could be wrong. Nevertheless, it is conventional to quote measurement accuracies in the VLF band and below in the language of a stochastic background: the fraction $\Omega_g(f)$ of the energy required to close the universe that lies in a bandwidth $\Delta f = f$ centered on frequency f. The current 95%-confidence limit on Ω_g from pulsar timing in the VLF band is $\Omega_g(4\times10^{-9}\ \text{Hz}) < 6\times10^{-8}H^{-2}$ where H is the Hubble constant in units of 100 km sec^{-1} Mpc^{-1} (Ref. 9). This is a sufficiently tight limit that is beginning to cast doubt on the (not terribly popular) suggestion that the universe contains enough vibrating loops of cosmic string for their gravitational pulls to have seeded galaxy formation.[10,11]

2.4 Extremely-Low-Frequency Band, 10^{-15} to 10^{-18} Hz

Gravitational waves in the extremely-low-frequency band (ELF), 10^{-15} to 10^{-18} Hz, should produce anisotropies in the cosmic microwave background radiation. The tightest limit from microwave observations comes from the lower edge of the ELF band $f \sim 10^{-18}$ Hz, where the gravitational wavelength is about π times the Hubble distance, and the waves, by squeezing all of the space inside our cosmological horizon in one direction and stretching it all in another, should produce a quadrupolar anisotropy in the microwave background. The quadrupolar anisotropy measured by the COBE satellite, if due primarily to gravitational waves (which it could be),[12,13] corresponds to an energy density $\Omega_g(10^{-18}\ \mathrm{Hz}) \sim 10^{-9}$. In Sec. 9, I shall discuss the implications of this impressive ELF limit for the strength of the early-universe stochastic background in the HF and LF bands.

2.5 Other Frequency Bands and Other Detection Methods

A large number of other methods have been conceived for searching for gravitational radiation. Some of them would operate best in the HF, LF, VLF, and ELF bands described above; others would operate best at other frequencies. However, none has shown anywhere near the promise or the achievements of the methods described above (laser interferometry on Earth and in space, resonant mass antennas, Doppler tracking of spacecraft, timing of pulsars, and anisotropy of microwave background). For some references to other methods, see, e.g., Ref. 6.

3 Ground-Based Laser Interferometers

3.1 Wave Polarizations, Waveforms, and How an Interferometer Works

According to general relativity theory (which I shall assume to be correct in this paper), a gravitational wave has two linear polarizations, conventionally called + (plus) and × (cross). Associated with each polarization, there is a gravitational-wave field, h_+ or $h_\times$, which oscillates in time and propagates with the speed of light. Each wave field produces tidal forces (stretching and squeezing forces) on any object or detector through which it passes. If the object is small compared to the waves' wavelength (as is the case for ground-based interferometers and resonant mass antennas), then relative to the object's center, the forces have the quadrupolar patterns shown in Fig. 1. The names "plus" and "cross" are derived

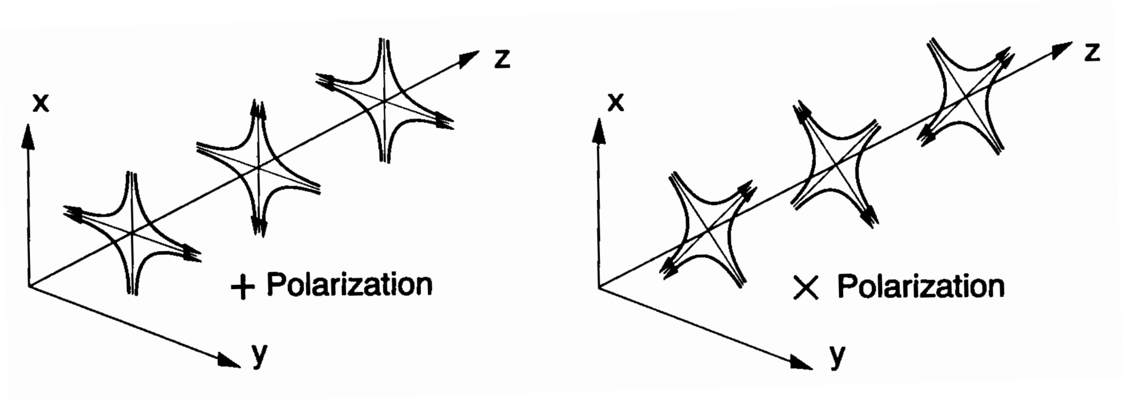

Figure 1: The lines of force associated with the two polarizations of a gravitational wave. (From Ref. 14.)

from the orientations of the axes that characterize the force patterns.[6]

A laser interferometer gravitational wave detector ("interferometer" for short) consists of four masses that hang from vibration-isolated supports as shown in Fig. 2, and the indicated optical system for monitoring the separations between the masses.[6,14] Two masses are near each other, at the corner of an "L," and one mass is at the end of each of the L's long arms. The arm lengths are nearly equal, $L_1 \simeq L_2 = L$. When a gravitational wave, with high frequencies compared to the masses' ~ 1 Hz pendulum frequency, passes through the detector, it pushes the masses back and forth relative to each other as though they were free from their suspension wires, thereby changing the arm-length difference, $\Delta L \equiv L_1 - L_2$. That change is monitored by laser interferometry in such a way that the variations in the output of the photodiode (the interferometer's output) are directly proportional to $\Delta L(t)$.

If the waves are coming from overhead or underfoot, and the axes of the + polarization coincide with the arms' directions, then it is the waves + polarization that drives the masses, and $\Delta L(t)/L = h_+(t)$. More generally, the interferometer's output is a linear combination of the two wave fields:

$$\frac{\Delta L(t)}{L} = F_+ h_+(t) + F_\times h_\times(t) \equiv h(t) \ . \tag{2}$$

The coefficients F_+ and $F_\times$ are of order unity and depend in a quadrupolar manner on the direction to the source and the orientation of the detector.[6] The combination $h(t)$ of the two h's is called the *gravitational-wave strain* that acts on the detector; and the time evolutions of $h(t)$, $h_+(t)$, and $h_\times(t)$ are sometimes called *waveforms*.

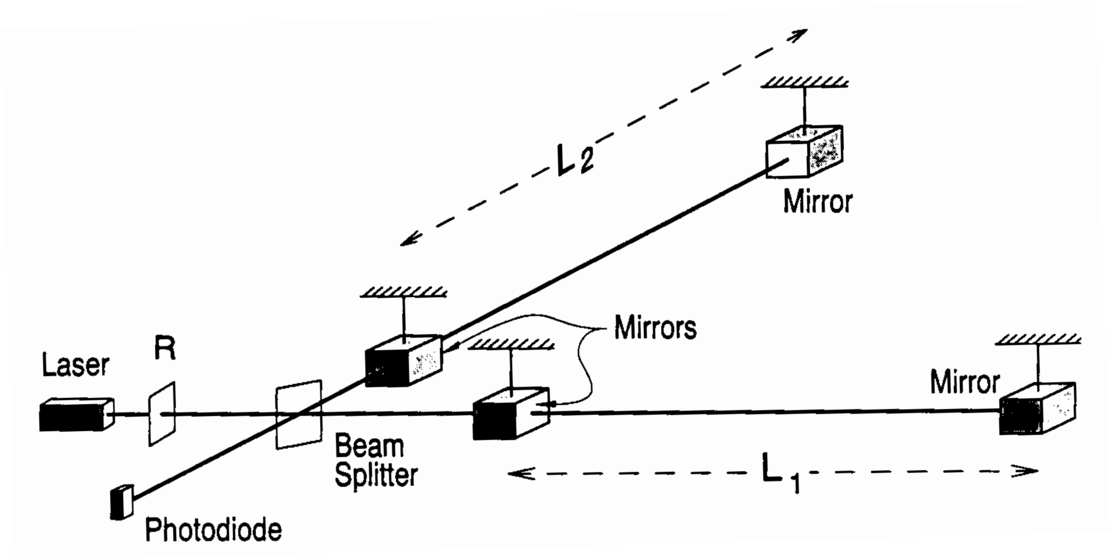

Figure 2: Schematic diagram of a laser interferometer gravitational wave detector. (From Ref. 14.)

Interferometer test masses at present are made of transparent fused silica, though other materials might be used in the future. The masses' inner faces (shown white in Fig. 2) are covered with high-reflectivity dielectric coatings to form the indicated "mirrors," while the masses' outer faces are covered with anti-reflection coatings. The two mirrors facing each other on each arm form a Fabry-Perot cavity. A beam splitter splits a carefully prepared laser beam in two and directs the resulting beams down the two arms. Each beam penetrates through the antireflection coating of its arm's corner mass, through the mass, and through the dielectric coating (the mirror); and thereby—with the length of the arm's Fabry-Perot cavity adjusted to be nearly an integral number of half wavelengths of light—the beam gets trapped in the cavity. The cavity's end mirror has much higher reflectivity than its corner mirror, so the trapped light leaks back out through the corner mirror and then hits the beam splitter where it recombines with light from the other arm. Most of the recombined light goes back toward the laser (where it can be returned to the interferometer by a "light-recycling mirror" labeled R), but a tiny portion goes toward the photodiode.

When a gravitational wave hits the detector and moves the masses, thereby changing the lengths L_1 and L_2 of the two cavities, it shifts each cavity's resonant frequency slightly relative to the laser frequency, and thereby changes the phase of the light in the cavity and the phase of the light that exits from the cavity toward the beam splitter. Correspondingly, the relative phase of the two beams returning to the splitter is altered by an amount $\Delta\Phi \propto \Delta L$, and this relative phase shift causes a change in the intensity of the recombined light at the photodiode, $\Delta I_{\rm pd} \propto \Delta\Phi \propto \Delta L \propto h(t)$. Thus, the change of photodiode output current is directly proportional to the gravitational-wave strain $h(t)$. This method of monitoring $h(t)$, which was invented by Ronald Drever[15] as a modification of Rainer Weiss's[16] seminal concept for such an interferometer, is capable of very high sensitivity, as we shall see below.

3.2 Wave Strengths and Interferometer Arm Lengths

The strengths of the waves from a gravitational-wave source can be estimated using the "Newtonian/quadrupole" approximation to the Einstein field equations. This approximation says that $h \simeq (G/c^4)\ddot{Q}/r$, where $\ddot{Q}$ is the second time derivative of the source's quadrupole moment, r is the distance of the source from Earth (and G and c are Newton's gravitation constant and the speed of light). The strongest sources will be highly nonspherical, and thus, will have $Q \simeq ML^2$ where M is their mass and L their size, and correspondingly, will have $\ddot{Q} \simeq 2Mv^2 \simeq 4E^{\rm ns}_{\rm kin}$ where v is their internal velocity and $E^{\rm ns}_{\rm kin}$ is the nonspherical part of their internal kinetic energy. This provides us with the estimate

$$h \sim \frac{1}{c^2}\frac{4G(E^{\rm ns}_{\rm kin}/c^2)}{r} \; ; \tag{3}$$

that is, h is about four times the gravitational potential produced at Earth by the mass-equivalent of the source's nonspherical, internal kinetic energy—made dimensionless by dividing by c^2. Thus, in order to radiate strongly, the source must have a very large, nonspherical, internal kinetic energy.

The best known way to achieve a huge internal kinetic energy is via gravity; and by energy conservation (or the virial theorem), any gravitationally-induced kinetic energy must be of the order of the source's gravitational potential energy. A huge potential energy, in turn, requires that the source be very compact, not much larger than its own gravitational radius. Thus, the strongest gravity-wave sources must be highly compact, dynamical concentrations of large amounts of mass (e.g., colliding and coalescing black holes and neutron stars).

Such sources cannot remain highly dynamical for long; their motions will be stopped by energy loss to gravitational waves and/or the formation of an allencompassing black hole. Thus, the strongest sources should be transient. Moreover, they should be very rare—so rare that to see a reasonable event rate will require reaching out through a substantial fraction of the universe. Thus, just as the strongest radio waves arriving at Earth tend to be extragalactic, so also the strongest gravitational waves are likely to be extragalactic.

For highly compact, dynamical objects that radiate in the high-frequency band, e.g., colliding and coalescing neutron stars and stellar-mass black holes, the internal, nonspherical kinetic energy $E_{\rm kin}^{\rm ns}/c^2$ is of the order of the mass of the Sun; and, correspondingly, Eq. (3) gives $h \sim 10^{-22}$ for such sources at the Hubble distance (3000 Mpc, i.e., 10^{10} light years); $h \sim 10^{-21}$ at 200 Mpc (a best-guess distance for several neutron-star coalescences per year; see Sec. 5.2), $h \sim 10^{-20}$ at the Virgo cluster of galaxies (15 Mpc); and $h \sim 10^{-17}$ in the outer reaches of our own Milky Way galaxy (20 kpc). These numbers set the scale of sensitivities that ground-based interferometers seek to achieve: $h \sim 10^{-21}$ to 10^{-22}.

When one examines the technology of laser interferometry, one sees good prospects to achieve measurement accuracies $\Delta L \sim 10^{-16}$ cm (1/1000 the diameter of the nucleus of an atom). With such an accuracy, an interferometer must have an arm length $L = \Delta L/h \sim 1$ to 10 km in order to achieve the desired wave sensitivities, 10^{-21} to 10^{-22}. This sets the scale of the interferometers that are now under construction.

3.3 LIGO, VIRGO, and the International Interferometric Network

Interferometers are plagued by non-Gaussian noise, e.g., due to sudden strain releases in the wires that suspend the masses. This noise prevents a single interferometer, by itself, from detecting with confidence short-duration gravitational-wave bursts (though it might be possible for a single interferometer to search for the periodic waves from known pulsars). The non-Gaussian noise can be removed by cross correlating two, or preferably three or more, interferometers that are networked together at widely separated sites.

The technology and techniques for such interferometers have been under development for nearly 25 years, and plans for km-scale interferometers have been developed over the past 14 years. An international network consisting of three km-scale interferometers, at three widely separated sites, is now in the early stages

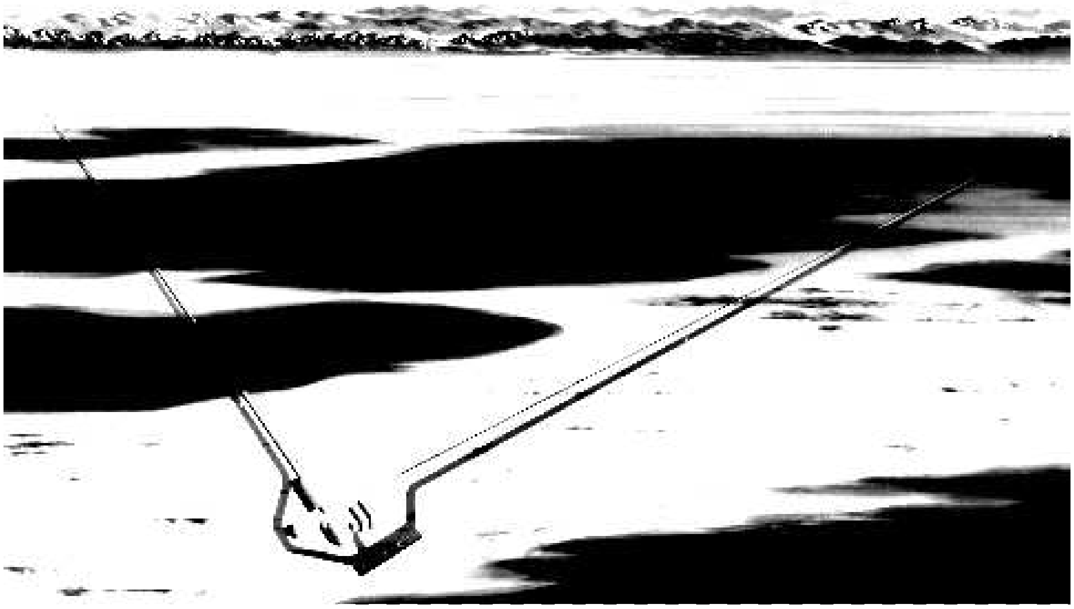

Figure 3: Artist's conception of one of the LIGO interferometers. (Courtesy of the LIGO Project.)

of construction. It includes two sites of the American LIGO Project ("Laser Interferometer Gravitational Wave Observatory")[14] and one site of the French/Italian VIRGO Project (named after the Virgo cluster of galaxies).[17]

LIGO will consist of two vacuum facilities with four-kilometer-long arms, one in Hanford, Washington (in the northwestern United States, Fig. 3) and the other in Livingston, Louisiana (in the southeastern United States). These facilities are designed to house many successive generations of interferometers without the necessity of any major facilities upgrade; and after a planned future expansion, they will be able to house several interferometers at once, each with a different optical configuration optimized for a different type of wave (e.g., broad-band burst, narrow-band periodic wave, or stochastic wave). The LIGO facilities and their first interferometers are being constructed by a team of about 80 physicists and engineers at Caltech and MIT, led by Barry Barish (the PI) and Gary Sanders (the Project Manager). Robbie Vogt (who directed the project during the preconstruction phase) is in charge of the final design and construction of LIGO's first interferometers, Stan Whitcomb is in charge of interferometer R&D, Albert Lazzarini is the system engineer, and Rai Weiss is the cognizant scientist for integration of all parts of LIGO.

A number of other research groups are making important contributions to LIGO: Bob Byer's group at Stanford is developing Nd:YAG lasers, Peter Saulson's group at Syracuse and Vladimir Braginsky's group in Moscow are developing test-mass suspension systems and studying noise in them, Jim Faller's group at JILA is developing active vibration isolation systems, Ron Drever's group at Caltech is developing advanced interferometers, and Sam Finn's group at Northwestern and my group at Caltech are developing data analysis techniques. A number of other groups are likely to join the LIGO effort in the next few years. A formal association of LIGO-related scientists (the *LIGO Research Community*, an analog of a "user's group" in high-energy physics) is being organized, and a LIGO Program Advisory Committee will be formed soon, with voting membership restricted to people outside the Caltech/MIT LIGO team, to advise the LIGO management.

The VIRGO Project is building one vacuum facility in Pisa, Italy, with three-kilometer-long arms. This facility and its first interferometers are a collaboration of more than a hundred physicists and engineers at the INFN (Frascati, Napoli, Perugia, Pisa), LAL (Orsay), LAPP (Annecy), LOA (Palaiseau), IPN (Lyon), ESPCI (Paris), and the University of Illinois (Urbana), under the leadership of Alain Brillet and Adalberto Giazotto.

Both LIGO and VIRGO are scheduled for completion in the late 1990s, and their first gravitational-wave searches are likely to be performed in 2000 or 2001.

LIGO alone, with its two sites which have parallel arms, will be able to detect an incoming gravitational wave, measure one of its two waveforms, and (from the time delay between the two sites) locate its source to within a $\sim 1^\circ$ wide annulus on the sky. LIGO and VIRGO together, operating as a *coordinated international network*, will be able to locate the source (via time delays plus the interferometers' beam patterns) to within a two-dimensional error box with size between several tens of arcminutes and several degrees, depending on the source direction and on the amount of high-frequency structure in the waveforms. They will also be able to monitor both waveforms $h_+(t)$ and $h_\times(t)$ (except for frequency components above about 1 kHz and below about 10 Hz, where the interferometers' noise becomes severe).

The accuracies of the direction measurements and the ability to monitor more than one waveform will be severely compromised when the source lies anywhere near the plane formed by the three LIGO/VIRGO interferometer locations. To get good all-sky coverage will require a fourth interferometer at a site far out of that plane; Japan and Australia would be excellent locations, and research groups there are carrying out research and development on interferometric detectors aimed at such a possibility. A 300-meter prototype interferometer called TAMA is under construction in Tokyo, and a 400-meter prototype called AIGO400 has been proposed for construction north of Perth.

Two other groups are major players in this field, one in Britain led by James Hough, the other in Germany, led by Karsten Danzmann. These groups each have two decades of experience with prototype interferometers (comparable experience to the LIGO team and far more than anyone else) and great expertise. Frustrated by inadequate financing for a kilometer-scale interferometer, they are constructing, instead, a 600-meter system called GEO600 near Hannover, Germany. Their goal is to develop, from the outset, an interferometer with the sort of advanced design that LIGO and VIRGO will attempt only as a "second-generation" instrument, and thereby achieve sufficient sensitivity to be full partners in the international network's first gravitational-wave searches; they then would offer a variant of their interferometer as a candidate for second-generation operation in the much longer arms of LIGO and/or VIRGO. It is a seemingly audacious plan, but with their extensive experience and expertise, the British/German collaboration might pull it off successfully.

3.4 Interferometer Development and Noise Sources

It is not possible, in the short vacuum systems now available (arm lengths ≤ 40 m), to develop and test a multikilometer interferometer as a single unit. This is because the various noise sources that plague an interferometer scale differently from each other with length L and with gravity-wave frequency f. As a result, the various components of the multikilometer interferometers, and the various techniques to be used in them, are being developed and tested separately in a number of different laboratories and will only be combined together into a single interferometer when the LIGO/VIRGO vacuum systems are completed.

The best known of the LIGO-Project laboratories in which components and techniques are being developed is the 40-meter prototype interferometer at Caltech (Fig. 4). This prototype focuses on the development of methods and components to control "displacement noise," i.e., those noise sources that push the mirrored test masses back and forth as would a gravity wave. The principal sources of

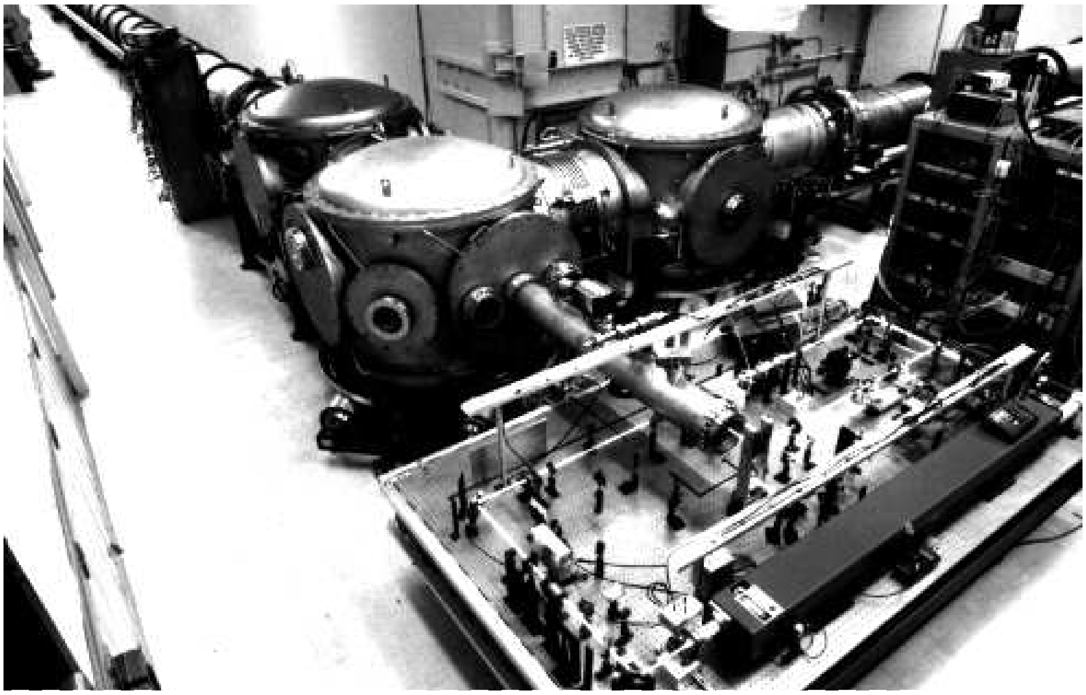

Figure 4: The LIGO Project's 40-meter "Mark II" prototype interferometer at Caltech. This prototype went into operation in 1993. It has much larger vacuum chambers, to accommodate bigger and better seismic isolation stacks, than those of the previous "Mark I" prototype (which operated from the early 1980s to 1992). [Courtesy of the LIGO Project.]

displacement noise are *seismic vibrations* of the ground beneath the interferometer (which are filtered out by the masses' suspension wires and by "isolation stacks" made of successive layers of steel and rubber), and *thermally-induced vibrations* of the test masses and of the wires that suspend them (vibrations that are controlled by designing the test masses and suspensions with great care and constructing them from low-loss, i.e., high "Q," materials).

Among the LIGO Project's other laboratories, there is a shorter-armed prototype interferometer facility at MIT, which is devoted to developing methods and components for controlling noise in the phase of the interferometer's light beams. Since the gravity wave makes itself known by the phase shift that it puts on the light of one interferometer arm relative to the other, this phase noise can simulate a gravity wave. Among the various causes of phase noise, the one that is the most fundamental is *photon shot noise* due to the random times at which the light's photons arrive at the photodiode (cf. Fig. 2).

Once the myriad of other noise sources have been brought under control, *shot noise*, *thermal noise* (i.e., thermally induced vibrations), and *seismic noise* (i.e., ground vibrations) are likely to be the ultimate impediments to detecting and studying gravitational waves. Figure 5 shows the spectra expected for each of these three noises in the first interferometers that will operate in LIGO. At frequencies above 200 Hz, shot noise dominates; between 200 Hz and 40 Hz, thermal noise in the suspension wires dominates; and below 40 Hz, seismic noise dominates.

During LIGO's operations, step-by-step improvements will be made in the control of these three noise sources,[14] thereby pushing the overall noise spectrum downward from the "first interferometer" level toward the "advanced interferometer" level shown in Fig. 5. As we shall see below, the sensitivity of the first interferometers might be inadequate to detect gravitational waves. However, we are quite confident that at some point during the improvement from first interferometers to advanced, a plethora of gravitational waves will be found and will start bringing us exciting information about fundamental physics and the universe.

Notice from Fig. 5 that the advanced LIGO interferometers are expected to have their optimal sensitivity at $f \sim 100$ Hz and rather good sensitivity all the way from $f \sim 10$ Hz at the low-frequency end to $f \sim 500$ Hz at the high-frequency end. Below 10 Hz, seismic noise, creeping through the isolation stacks, will overwhelm all gravitational-wave signals; and above 500 Hz, photon shot noise may overwhelm the signals.

Figure 6 gives an impression of the present state of interferometer technology and the rate of progress. This figure shows a sequence of noise spectra in the 40-meter prototype interferometer at Caltech during 1990–94, when the 40-meter R&D emphasis was on improving the low-frequency noise performance. The top two (noisiest) spectra are snapshots of the original "Mark I" prototype performance in October 1990 and June 1992; the lower two (quieter) spectra are from the rebuilt, "Mark II" prototype of Fig. 4, in March and October 1994. The smooth, solid line, for comparison, is the displacement noise goal for the first 4-km interferometers in LIGO (i.e., it is the upper solid curve of Fig. 5).

Note that the prototypes's arm-length difference was being monitored, in October 1994, to within an rms noise level (in a bandwidth equal to frequency) $\Delta L_{\rm rms} = \sqrt{f}\Delta\tilde{L}(f) < 8 \times 10^{-16}$ cm over the frequency range 200 to 1000 Hz. This corre-

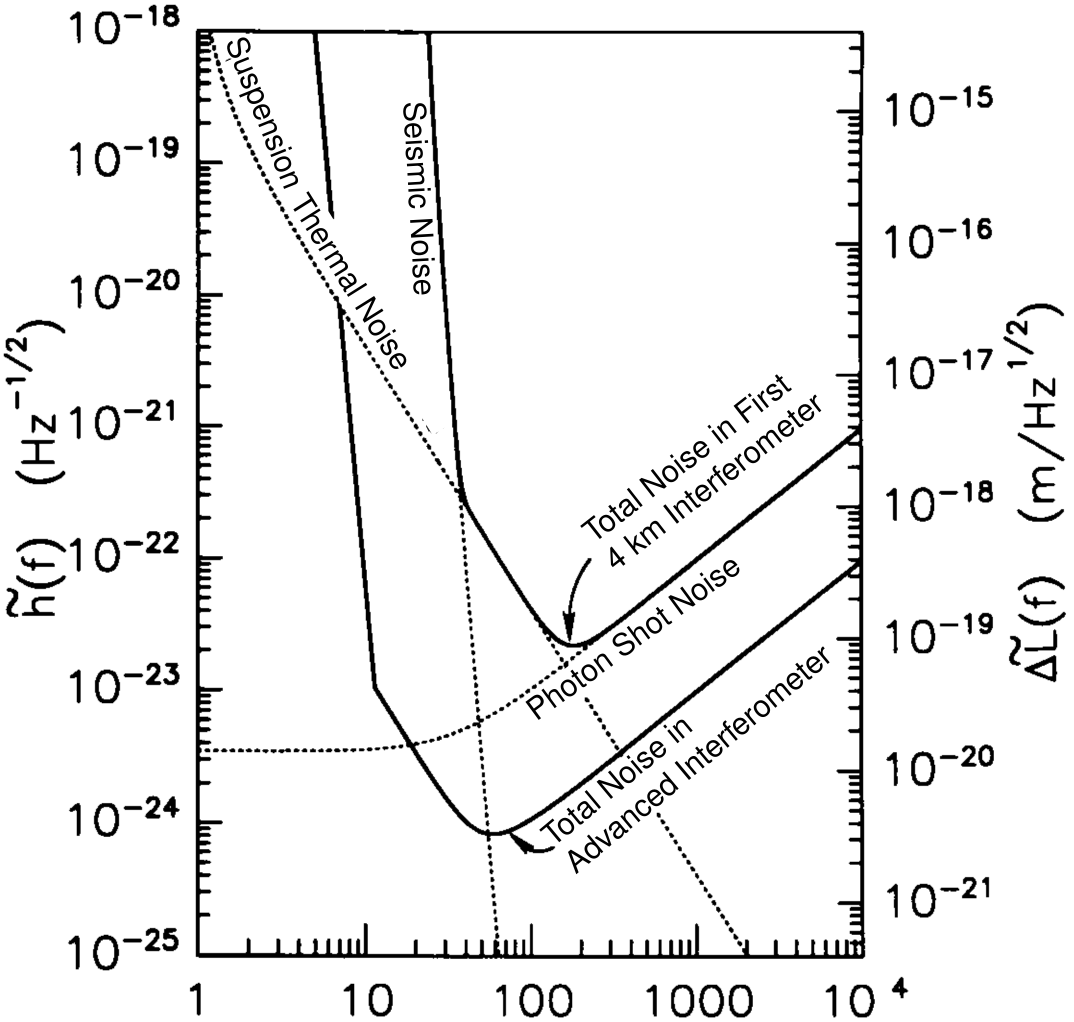

Figure 5: The expected noise spectrum in each of LIGO's first 4-km interferometers (upper solid curve) and in more advanced interferometers (lower solid curve). The dashed curves show various contributions to the first interferometers' noise. Plotted horizontally is gravity-wave frequency f; plotted vertically is $\tilde{h}(f)$, the square root of the spectral density of the detector's output $h(t) = \Delta L(t)/L$ in the absence of a gravity wave. The rms h noise in a bandwidth Δf at frequency f is $h_{\rm rms} = \tilde{h}(f)\sqrt{\Delta f}$. (From Ref. 14.)

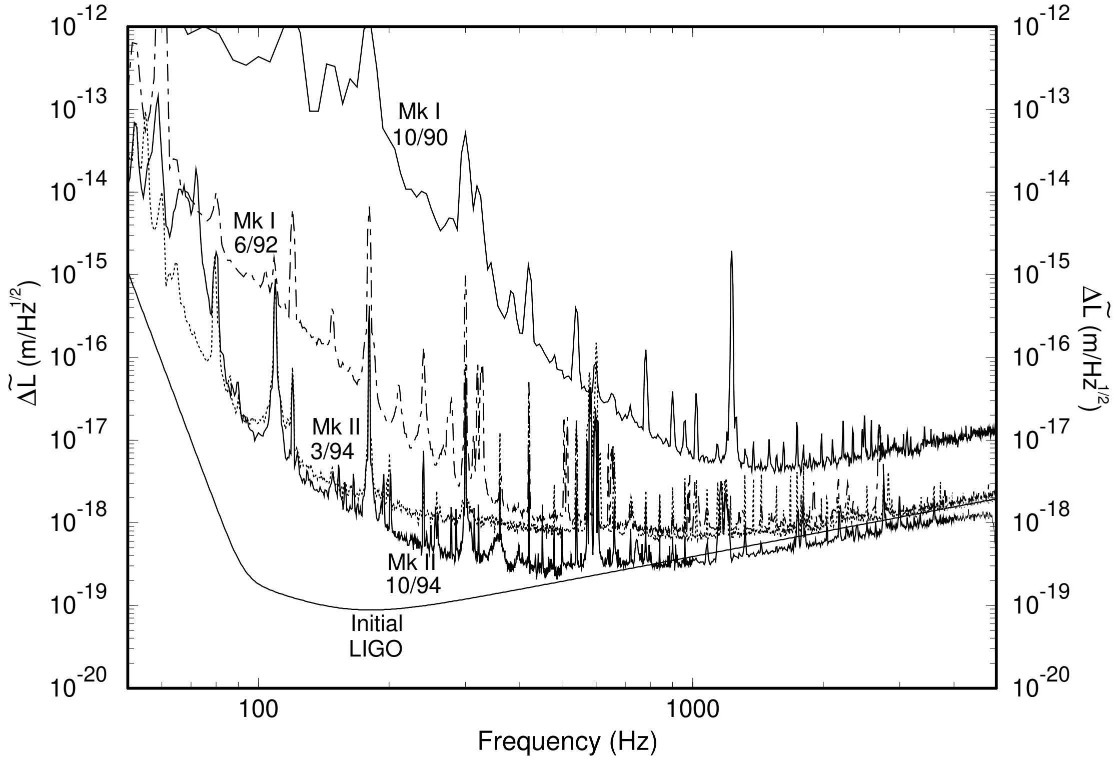

Figure 6: Measured noise spectra in the Caltech 40-meter prototype interferometer (Fig. 4). Since this prototype is devoted to learning to control displacement noise, the spectra shown are $\Delta\tilde{L}(f)$, the square root of the spectral density of the measured arm-length difference. Each of the many spectral lines is well understood, and most could be removed if their removal were of high priority (e.g., they are multiples of the 60 Hz line frequency sneaking into the apparatus by known routes). Those few, very narrow lines that cannot be physically removed by cleaning up the instrument (e.g., thermally-driven violin-mode resonances of the wires that suspend the test masses) will be filtered out in the data analysis. Thus, the interferometer sensitivity is characterized by the continuum noise floor and not the lines. (From Ref. 18.)

sponds to an rms gravitational-wave noise level $h_{\rm rms} = \Delta L_{\rm rms}/40$ m $< \ 2 \times 10^{-19}$, the best that any gravitational-wave detector has yet achieved.

3.5 Semiquantitative Discussion of Interferometer Noise

The LIGO and VIRGO interferometers are expected to have rms noise levels $h_{\rm rms} \lesssim 10^{-22}$ corresponding to test-mass position noises $\Delta L_{\rm rms} \lesssim hL \sim 10^{-16}$ cm. 10^{-16} cm is awfully small: 1/1000 the diameter of the nucleus of an atom, and 10^{-12} the wavelength of the light being used to monitor the masses' motions. How can one possibly monitor such small motions? The following estimate explains how.

One adjusts the reflectivities of the interferometer's corner mirrors so the two arms store the laser light on average for about half a cycle of a ~ 100 Hz gravitational wave, which means for ~ 100 round trips. The light in each arm thereby acquires a phase shift

$$\Delta\Phi \sim 100 \times 4\pi\Delta L/\lambda \sim 10^{-9} \ , \tag{4}$$

where $\lambda \sim 10^{-4}$ cm is the wavelength of light. If the interference of the light from the two beams is done optimally, then this phase shift (equal and opposite in the two arms) can be measured at the photodiode to an accuracy that is governed by the light's photon shot noise, $\Delta\Phi \sim 1/\sqrt{N}$, where N is the number of photons that enter the interferometer from the laser during the half-cycle of photon storage time. (This $1/\sqrt{N}$ is the usual photon fluctuation in a quantum mechanical "coherent state" of light.) Thus, to achieve the required accuracy, $\Delta\Phi \sim 10^{-9}$, in the face of photon shot noise, requires $N \sim 10^{18}$ photons in 0.01 second, which means a laser power of ~ 100 Watts.

By cleverness,[15] one can reduce the required laser power. The light is stored in the interferometer arms for only a half gravity-wave period (~ 100 round trips) because during the next half period, the waves would reverse the sign of ΔL, thereby reversing the sign of the phase shift being put onto the light and removing from the light the signal that had accumulated in the first half period. In just 100 round trips, however, the light is attenuated hardly at all. One therefore reuses the light, over and over again. This is done by (1) operating the interferometer with only a tiny fraction of the recombined light going out toward the photodiode, and almost all of it instead going back toward the laser, and by (2) placing a mirror (marked R in Fig. 2) between the laser and the interferometer in just such a position that the entire interferometer becomes an optical cavity driven by the laser—with its arms as two subcavities. Then the mirror R recycles the recombined light back into the interferometer in phase with the new laser light, thereby enabling a laser of, say, 5 Watts to behave like one of 100 Watts or more.

Let's turn from photon shot noise to thermal noise. How, one might ask, can one possibly expect to monitor the mirrors' motions at a level of 10^{-16} cm when the room-temperature atoms of which the fused-silica mirrors are made vibrate thermally with amplitudes $\Delta l_{\rm rms} = \sqrt{kT/m\omega^2} \sim 10^{-10}$ cm? (Here k is Boltzmann's constant, T is room temperature, m is the atomic rest mass, and $\omega \sim 10^{14}$ s^{-1} is the angular frequency of atomic vibration.) The answer is that these individual atomic vibrations are unimportant. The light beam, with its ~ 5 cm diameter, averages over the positions of $\sim 10^{17}$ atoms in the mirror, and with its 0.01 s storage time, it averages over $\sim 10^{11}$ vibrations of each atom. This spatial and temporal averaging makes the vibrations of individual atoms irrelevant. Not so irrelevant, however, are the lowest-frequency normal-mode vibrations of the mirror-endowed masses (since these modes experience much less time averaging than the faster atomic vibrations). Assuming a mass $m \sim$ (a few tens of kg), these normal modes have angular frequencies $\omega \sim 10^5$ s^{-1}, so their rms vibration amplitude is $\Delta l_{\rm rms} = \sqrt{kT/m\omega^2} \sim 10^{-14}$ cm. This is 100 times larger than the signals we wish to monitor; but if these modes have high quality factors (high Q's; low losses), then the vibrations will be very steady over the interferometer's averaging time of 0.01 s, and correspondingly, their effects will average down by more than a factor of 100. Similar considerations apply to the thermal noise in the masses' suspension wires. For detailed discussions of fascinating and not-fully-understood physics issues that influence the thermal noise, see, e.g., Refs. 19-21.

At the LIGO sites, and most any other quiet location on Earth, the ground is continually shaking with an rms displacement $\Delta l_{\rm rms} \sim 10^{-8}$ cm $(100 \text{ Hz}/f)^{3/2}$. This is 10^7 times larger than the motions one seeks to monitor. At frequencies above 10 Hz or so, one can protect the masses from these seismic vibrations by simple (but carefully designed) passive isolation stacks. Each element in the stack is a mass and a spring (a harmonic oscillator) with normal-mode frequency $f_0 \sim$ (a few Hz). When seismic noise tries to drive this harmonic oscillator far above its resonant frequency [in our case, at $f \gtrsim$ (a few tens of Hz)], the amplitude of its response is attenuated relative to the driving motion by a factor $(f_0/f)^2$ [in our

Figure 7: The seismic isolation stack that was recently installed in the LIGO Project's Mark II prototype interferometer at Caltech. When the interferometer is in operation, a small tower is mounted on the top steel plate and from the tower hangs one of the interferometer's mirror-endowed masses. [Courtesy of the LIGO Project.]

case, a factor $\gtrsim 10^2$]. Thus, each oscillator in the stack will provide a reduction $\gtrsim 10^2$ in $\Delta l_{\rm rms}$, so a stack of four or five oscillators is enough to provide the required isolation. Figure 7 shows an isolation stack—made of four steel plates and four sets of Viton rubber springs (not quite visible between the plates)—that is now operating in the Mark II prototype interferometer of Fig. 4. This stack and the pendulum wires that suspend the mirror-endowed test masses provide five layers of isolation. The installation of this new stack was responsible for the sharp drop in low-frequency noise in Fig. 6 between June 1992 (Mark I) and March 1994 (Mark II).

The above rough estimates suggest (as Weiss realized as early as 1972)[16] that it is possible for interferometers to achieve the required sensitivities, $h_{\rm rms} \sim 10^{-22}$ and $\Delta L \sim 10^{-16}$ cm. However, going from these rough estimates to a real working interferometer, and doing so in the face of a plethora of other noise sources, is a tremendous experimental challenge—one that has occupied a number of excellent experimental physicists since 1972.

4 Resonant-Mass Antennas

A resonant-mass antenna for gravitational radiation consists of a solid body that (heuristically speaking) rings like a bell when a gravitational wave hits it. This body (the resonant mass) is usually a cylinder, but future variants are likely to be spheres or sphere-like, e.g., a truncated icosahedron gravitational-wave antenna or TIGA.[22] The resonant mass is typically made from an alloy of aluminum and weighs several tons, but some have been made of niobium or single-crystal silicon or sapphire (but with masses well below a ton). To control thermal noise, the resonant mass is usually cooled cryogenically to liquid-helium temperatures or below.

The resonant-mass antenna is instrumented with an electromagnetic transducer and electronics, which monitor the complex amplitude of one or more of the mass's normal modes. When a gravitational wave passes through the mass, its frequency components near each normal-mode frequency f_o drive that mode, changing its complex amplitude; and the time evolution of the changes is measured within some bandwidth Δf by the transducer and electronics. Current resonant-mass antennas are narrow-band devices ($\Delta f/f_o \ll 1$) but in the era of LIGO/VIRGO, they might achieve bandwidths as large as $\Delta f/f_o \sim 1/3$.

Resonant-mass antennas for gravitational radiation were pioneered by Joseph Weber about 35 years ago[23] and have been pushed to ever higher sensitivity by Weber and a number of other research groups since then. For references and an overview of the present and future of such antennas, see, e.g., Ref. 24. At present, there is a network of such antennas,[25] cooled to 3 K, and operating with an rms noise level for broad-band gravity-wave bursts of $h_{\rm rms} \simeq 6\times10^{-19}$. The network includes an aluminum cylinder called EXPLORER built by a group at the University of Rome, Italy (Edoardo Amaldi, Guido Pizella, *et al.*); an aluminum cylinder at Louisiana State University, United States (Bill Hamilton, Warren Johnson, *et al.*); and a niobium cylinder at the University of Perth, Australia (David Blair *et al.*). This network has been in operation, searching for waves, for several years.

The next generation of resonant-mass antennas is now under construction at the University of Rome (NAUTILUS) and at the University of Legarno, Italy (AURIGA). These are several-ton aluminum bars cooled to 0.05 K; their rms design sensitivities for wave bursts are (several)$\times10^{-20}$ (Ref. 24).

A subsequent generation, which hopefully would operate in the LIGO/VIRGO era, is being discussed and planned.[24] These are 1 to 100 ton spheres or TIGA's cooled to ~ 0.01–0.05 K, with sensitivity goals of $\sim 10^{-21}$. Such antennas might be built by an American collaboration, a Brazilian collaboration, an Italian collaboration called "Omega," and/or a Dutch collaboration called "Grail." Their spherical or near-spherical shapes make them omnidirectional and should give them several-times higher sensitivities than can be achieved by cylinders at the same frequency.

The attractiveness of such antennas in the LIGO/VIRGO era lies in their ability to operate with impressive sensitivity in the uppermost reaches of the high-frequency band, $\sim 10^3$ to 10^4 Hz, where photon shot noise debilitates the performance of interferometric detectors (cf. Fig. 5). Figure 8 shows the projected rms noise curves of a family of TIGA detectors, each instrumented to operate at the "standard quantum limit" for such a detector (a nontrivial experimental task). Shown for comparison is the rms noise of the first LIGO interferometer—which, of course, is not optimized for the kHz band. The GEO600 interferometer, with its advanced design, can be operated in a narrow-band, high-frequency mode (and probably will be so operated in $\sim$ 1999). Its rms design sensitivity in such a mode is also shown in Fig. 8. The TIGA sensitivities are sufficiently good in the kHz band, compared to early LIGO and GEO interferometers, so that although they probably cannot begin to operate until somewhat after the beginning of the LIGO/VIRGO era, they might be fully competitive when they do operate and might play an important role in the kHz band.

5 High-Frequency Gravitational-Wave Sources: Coalescing Compact Binaries

The best understood of all gravitational-wave sources are coalescing, compact binaries composed of neutron stars (NS) and black holes (BH). These NS/NS, NS/BH, and BH/BH binaries may well become the "bread and butter" of the LIGO/VIRGO diet.

The Hulse-Taylor[2,3] binary pulsar, PSR $1913+16$, is an example of a NS/NS binary whose waves could be measured by LIGO/VIRGO, if we were to wait long enough. At present, PSR $1913+16$ has an orbital frequency of about 1/(8 hours)

Figure 8: The rms noise curves $\tilde{h}(f)$ (measured in strain per root Hz) for a "xylaphone" of TIGA gravitational-wave detectors (solid curves) for signals of random polarization and direction.[22] The TIGA's are presumed instrumented and cooled sufficiently well that their sensitivity is at the standard quantum limit. Their central frequencies, radii, and masses (assuming aluminum material) are {1.0 kHz, 1.30 m, 25.1 ton}, {1.25 kHz, 1.04 m, 12.8 ton}, {1.50 kHz, 0.87 m, 7.4 ton}, {1.75 kHz, 0.74 m, 4.7 ton}, and {2.0 kHz, 0.65 m, 3.1 ton}. Shown for comparison are the noise curves for the first LIGO interferometer with random-wave polarization and direction multiplied by $\sqrt{5}$ (dotted curve; Fig. 5), and for the first GEO600 detector operated in a narrow-band mode (dashed curve; Ref. 26).

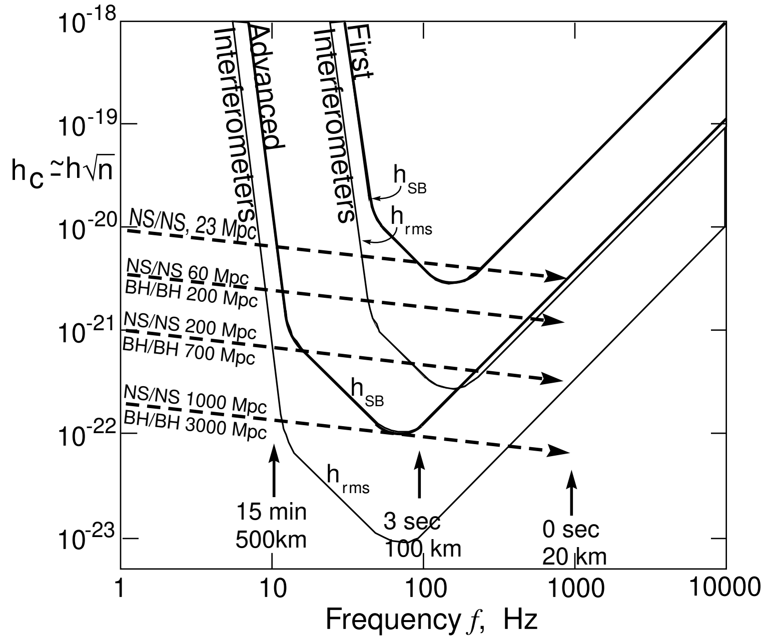

Figure 9: LIGO's projected broad-band noise $h_{\rm rms}$ and sensitivity to bursts $h_{\rm SB}$ (Fig. 5 and Ref. 14) compared with the strengths of the waves from the last few minutes of inspiral of compact binaries. The signal to noise ratios are $\sqrt{2}$ higher than in Ref. 14 because of a factor of two error in Eq. (29) of Ref. 6.

and emits its waves predominantly at twice this frequency, roughly 10^{-4} Hz, which is in the low-frequency band—far too low to be detected by LIGO/VIRGO. However, as a result of their loss of orbital energy to gravitational waves, the PSR $1913+16$ NS's are gradually spiraling inward. If we wait roughly 10^8 years, this inspiral will bring the waves into the LIGO/VIRGO high-frequency band. As the NS's continue their inspiral, the waves will then sweep upward in frequency, over a time of about 15 minutes, from 10 Hz to $\sim 10^3$ Hz, at which point the NS's will collide and coalesce. It is this last 15 minutes of inspiral, with $\sim 16{,}000$ cycles of waveform oscillation, and the final coalescence that LIGO/VIRGO seeks to monitor.

5.1 Wave Strengths Compared to LIGO Sensitivities

Figure 9 compares the projected sensitivities of interferometers in LIGO[14] with the wave strengths from the last few minutes of inspiral of BH/BH, NS/BH, and NS/NS binaries at various distances from Earth. The two solid curves at the bottoms of the stippled regions (labeled $h_{\rm rms}$) are the rms noise levels for broad-band waves that have optimal direction and polarization. The tops of the stippled regions (labeled $h_{\rm SB}$ for "sensitivity to bursts") are the sensitivities for highly confident detection of randomly polarized, broad-band waves from random directions (i.e., the sensitivities for high confidence that any such observed signal is not a false alarm due to Gaussian noise). The upper stippled region and its bounding curves are the expected performances of the first interferometers in LIGO; the lower stippled region and curves are performances of more advanced LIGO interferometers; cf. Fig. 5.

As the NS's and/or BH's spiral inward, their waves sweep upward in frequency (left to right in the diagram). The dashed lines show their "characteristic" signal strength h_c (approximately the amplitude h of the waves' oscillations multiplied by the square root of the number of cycles spent near a given frequency, $\sqrt{n}$); the signal-to-noise ratio is this h_c divided by the detector's $\sqrt{5}h_{\rm rms}$, $S/N = h_c/(\sqrt{5}h_{\rm rms})$, where the $\sqrt{5}$ converts $h_{\rm rms}$ from "optimal direction and polarization" to "random direction and polarization").[14,6] The arrows along the bottom inspiral track indicate the time until final coalescence for an NS/NS binary and the separation between the NS centers of mass. Each NS is assumed to have a mass of 1.4 suns and a radius $\sim$ 10 km, and for each BH, 10 suns and $\sim$ 20 km.

Notice that the signal strengths in Fig. 9 are in good accord with our rough estimates based on Eq. (3); at the endpoint (right end) of each inspiral, the number of cycles n spent near that frequency is of order unity, so the quantity plotted, $h_c \simeq h\sqrt{n}$, is about equal to h—and at distance 200 Mpc is roughly 10^{-21}, as we estimated in Sec. 3.2.

5.2 Coalescence Rates

Such final coalescences are few and far between in our own galaxy: about one every 100,000 years, according to 1991 estimates by Phinney[27] and by Narayan, Piran, and Shemi,[28] based on the statistics of binary pulsar searches in our galaxy which found three that will coalesce in less than 10^{10} years. Extrapolating out through the universe on the basis of the density of production of blue light (the color produced predominantly by massive stars), Phinney[27] and Narayan *et al.*[28] infer that to see several NS/NS coalescences per year, LIGO/VIRGO will have to look out to a distance of about 200 Mpc (give or take a factor of $\sim$ 2); cf. the

"NS/NS inspiral, 200 Mpc" line in Fig. 9. Since these estimates were made, the binary pulsar searches have been extended through a significantly larger volume of the galaxy than before, and no new ones with coalescence times $\lesssim 10^{10}$ years have been found; as a result, the binary-pulsar-search-based best estimate of the coalescence rate should be revised downward,[29] perhaps to as little as one every million years in our galaxy, corresponding to a distance 400 Mpc for several per year.[29]

A rate of one every million years in our galaxy is ~ 1000 times smaller than the birth rate of the NS/NS binaries' progenitors: massive, compact, main-sequence binaries.[27,28] Therefore, either 99.9% of progenitors fail to make it to the NS/NS state (e.g., because of binary disruption during a supernova or forming TŻO's), or else they do make it, but they wind up as a class of NS/NS binaries that has not yet been discovered in any of the pulsar searches. Several experts on binary evolution have argued for the latter:[30–32] Most NS/NS binaries, they suggest, may form with such short orbital periods that their lifetimes to coalescence are significantly shorter than normal pulsar lifetimes ($\sim 10^7$ years); and with such short lifetimes, they have been missed in pulsar searches. By modeling the evolution of the galaxy's binary star population, the binary experts arrive at best estimates as high as 3×10^{-4} coalescences per year in our galaxy, corresponding to several per year out to a 60-Mpc distance.[30] Phinney[27] describes other plausible populations of NS/NS binaries that could increase the event rate, and he argues for "ultraconservative" lower and upper limits of 23 Mpc and 1000 Mpc for how far one must look to see several coalescences per year.

By comparing these rate estimates with the signal strengths in Fig. 9, we see that (1) the first interferometers in LIGO/VIRGO have a possibility but not high probability of seeing NS/NS coalescences; (2) advanced interferometers are almost certain of seeing them (the requirement that this be so was one factor that forced the LIGO/VIRGO arm lengths to be so long, several kilometers); and (3) they are most likely to be discovered roughly half-way between the first and advanced interferometers—which means by an improved variant of the first interferometers several years after LIGO operations begin.

We have no good observational handle on the coalescence rate of NS/BH or BH/BH binaries. However, theory suggests that their progenitors might not disrupt during the stellar collapses that produce the NS's and BH's, so their coalescence rate could be about the same as the birth rate for their progenitors:

$\sim 1/100,000$ years in our galaxy. This suggests that within a 200 Mpc distance, there might be several NS/BH or BH/BH coalescences per year.[27,28,30,32] This estimate should be regarded as a plausible upper limit on the event rate and a lower limit on the distance to look.[27,28]

If this estimate is correct, then NS/BH and BH/BH binaries will be seen before NS/NS and might be seen by the first LIGO/VIRGO interferometers or soon thereafter; cf. Fig. 9. However, this estimate is far less certain than the (rather uncertain) NS/NS estimates!

Once coalescence waves have been discovered, each further improvement of sensitivity by a factor of two will increase the event rate by $2^3 \simeq 10$. Assuming a rate of several NS/NS per year at 200 Mpc, the advanced interferometers of Fig. 9 should see ~ 100 per year.

5.3 Inspiral Waveforms and the Information They Can Bring

Neutron stars and black holes have such intense self-gravity that it is exceedingly difficult to deform them. Correspondingly, as they spiral inward in a compact binary, they do not gravitationally deform each other significantly until several orbits before their final coalescence.[33,34] This means that the inspiral waveforms are determined to high accuracy by only a few, clean parameters: the masses and spin angular momenta of the bodies, and the initial orbital elements (i.e., the elements when the waves enter the LIGO/VIRGO band).

Though tidal deformations are negligible during inspiral, relativistic effects can be very important. If, for the moment, we ignore the relativistic effects—i.e., if we approximate gravity as Newtonian and the wave generation as due to the binary's oscillating quadrupole moment,[6] then the shapes of the inspiral waveforms $h_+(t)$ and $h_\times(t)$ are as shown in Fig. 10.

The left-hand graph in Fig. 10 shows the waveform increasing in amplitude and sweeping upward in frequency (i.e., undergoing a "chirp") as the binary's bodies spiral closer and closer together. The ratio of the amplitudes of the two polarizations is determined by the inclination, ι, of the orbit to our line of sight (lower right in Fig. 10). The shapes of the individual waves, i.e., the waves' harmonic content, are determined by the orbital eccentricity (upper right). (Binaries produced by normal stellar evolution should be highly circular due to past radia-

Figure 10: Waveforms from the inspiral of a compact binary, computed using Newtonian gravity for the orbital evolution and the quadrupole-moment approximation for the wave generation. (From Ref. 14.)

tion reaction forces, but compact binaries that form by capture events, in dense star clusters that might reside in galactic nuclei,[35] could be quite eccentric.) If, for simplicity, the orbit is circular, then the rate at which the frequency sweeps or "chirps," df/dt [or equivalently, the number of cycles spent near a given frequency, $n = f^2(df/dt)^{-1}$] is determined solely, in the Newtonian/quadrupole approximation, by the binary's so-called *chirp mass*, $M_c \equiv (M_1 M_2)^{3/5}/(M_1 + M_2)^{1/5}$ (where M_1 and M_2 are the two bodies' masses). The amplitudes of the two waveforms are determined by the chirp mass, the distance to the source, and the orbital inclination. Thus (in the Newtonian/quadrupole approximation), by measuring the two amplitudes, the frequency sweep, and the harmonic content of the inspiral waves, one can determine as direct, resulting observables, the source's distance, chirp mass, inclination, and eccentricity.[36,37]

As in binary pulsar observations,[3] so also here, relativistic effects add further information. They influence the rate of frequency sweep and produce waveform modulations in ways that depend on the binary's dimensionless ratio $\eta = \mu/M$ of reduced mass $\mu = M_1 M_2/(M_1 + M_2)$ to total mass $M = M_1 + M_2$[40] and on the spins of the binary's two bodies.[41] These relativistic effects are reviewed and discussed at length in Refs. 38 and 42. Two deserve special mention: (1) As the waves emerge from the binary, some of them get backscattered one or more times

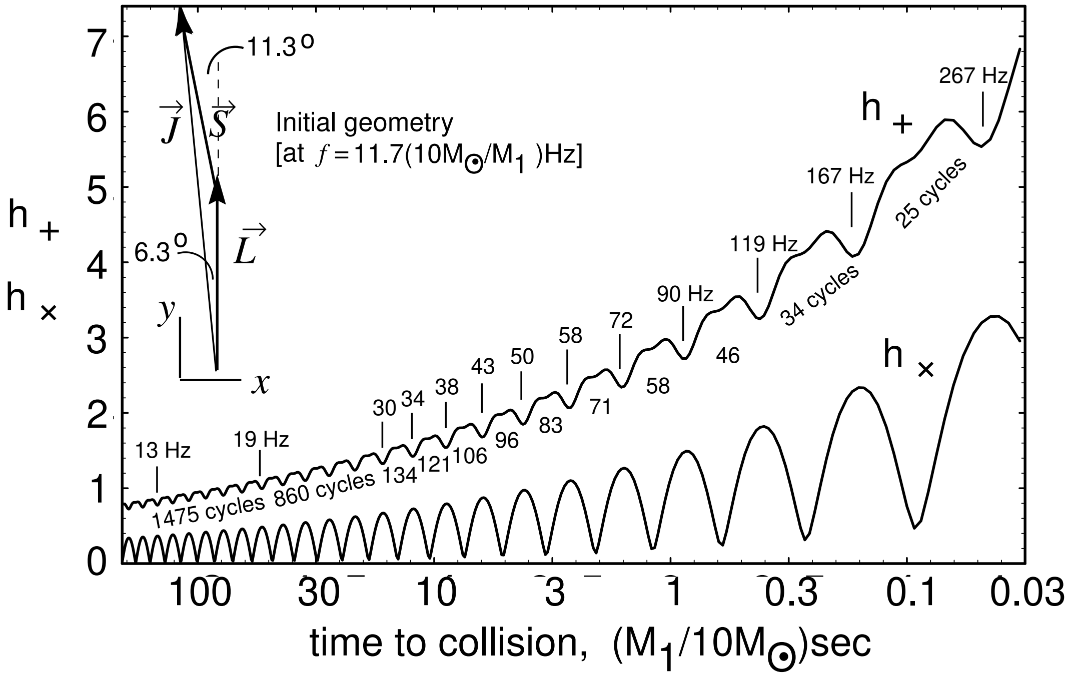

Figure 11: Modulational envelope for the waveform from a 1 $M_\odot$ nonspinning NS spiraling into a 10 $M_\odot$, rapidly spinning Kerr black hole (spin parameter $a = 1$). The orbital angular momentum L is inclined by $\alpha = 11.3^\circ$ to the hole's spin angular momentum S, and the two precess around $J = L + S$, whose direction remains fixed in space as $L = |L|$ shrinks and $S = |S| = M_{\rm BH}a$ remains constant. The precession modulates the waves by an amount that depends on (1) the direction to Earth (here along the initial $L \times S$, i.e., out of the paper) and (2) the orientation of the detector's arms (here parallel to the figure's initial L and to $L\times$(direction to Earth) for h_+, and rotated 45° for $h_\times$). The figure shows the waveforms' modulational envelopes (in arbitrary units, the same for h_+ and $h_\times$), parametrized by the wave frequency f and the number of cycles of *oscillation* between the indicated f's. The total number of *precessions* from f to coalescence is $N_{\rm prec} \simeq (5/64\pi)(Ma/\mu)(\pi M f)^{-2/3} \simeq 20(f/10\ {\rm Hz})^{-2/3}$. (From Refs. 38 and 39.)

off the binary's spacetime curvature, producing wave *tails*. These tails act back on the binary, modifying its inspiral rate in a measurable way. (2) If the orbital plane is inclined to one or both of the binary's spins, then the spins drag inertial frames in the binary's vicinity (the "lense-thirring effect"); this frame dragging causes the orbit to precess, and the precession modulates the waveforms.[38,39,43] Figure 11 shows the resulting modulation for a 1 $M_\odot$ NS spiraling into a rapidly spinning, 10 $M_\odot$ BH.

Remarkably, the relativistic corrections to the frequency sweep will be measurable with very high accuracy, even though they are typically $\lesssim 10\%$ of the Newtonian contribution, and even though the typical signal-to-noise ratio will be only ~ 9 even after optimal signal processing. The reason is as follows:[38,44,45] The frequency sweep will be monitored by the method of "matched filters"; in other words, the incoming, noisy signal will be cross correlated with theoretical templates. If the signal and the templates gradually get out of phase with each other by more than $\sim 1/10$ cycle as the waves sweep through the LIGO/VIRGO band, their cross correlation will be significantly reduced. Since the total number of cycles spent in the LIGO/VIRGO band will be $\sim 16,000$ for a NS/NS binary, ~ 3500 for NS/BH, and ~ 600 for BH/BH, this means that LIGO/VIRGO should be able to measure the frequency sweep to a fractional precision $\lesssim 10^{-4}$, compared to which the relativistic effects are very large. (This is essentially the same method as the one Joseph Taylor and colleagues use for high-accuracy radio-wave measurements of relativistic effects in binary pulsars.)[3]

Preliminary analyses, using the theory of optimal signal processing, predict the following typical accuracies for LIGO/VIRGO measurements based solely on the frequency sweep (i.e., ignoring modulational information):[38,44–47] (1) The chirp mass M_c will typically be measured, from the Newtonian part of the frequency sweep, to $\sim 0.04\%$ for a NS/NS binary and $\sim 0.3\%$ for a system containing at least one BH. (2) *If* we are confident (e.g., on a statistical basis from measurements of many previous binaries) that the spins are a few percent or less of the maximum physically allowed, then the reduced mass μ will be measured to $\sim 1\%$ for NS/NS and NS/BH binaries, and $\sim 3\%$ for BH/BH binaries. (Here and below, NS means a ~ 1.4 $M_\odot$ neutron star and BH means a ~ 10 $M_\odot$ black hole.) (3) Because the frequency dependences of the (relativistic) μ effects and spin effects are not sufficiently different to give a clean separation between μ and the spins, if we have no prior knowledge of the spins, then the spin/μ correlation will worsen the typical accuracy of μ by a large factor, to $\sim 30\%$ for NS/NS, $\sim 50\%$ for NS/BH, and a factor ~ 2 for BH/BH.[46,44] These worsened accuracies might be improved somewhat by waveform modulations caused by the spin-induced precession of the orbit,[39,43] and even without modulational information, a certain combination of μ and the spins will be determined to a few percent. Much additional theoretical work is needed to firm up the measurement accuracies.

To take full advantage of all the information in the inspiral waveforms will require theoretical templates that are accurate, for given masses and spins, to a fraction of a cycle during the entire sweep through the LIGO/VIRGO band. Such templates are being computed by an international consortium of relativity theorists (Blanchet and Damour in France, Iyer in India, Will and Wiseman in the United States, and others),[42,48] using post-Newtonian expansions of the Einstein field equations. This enterprise is rather like computing the Lamb shift to high order in powers of the fine structure constant, for comparison with experiment. The terms of leading order in the mass ratio $\eta = \mu/M$ are being checked by a Japanese-American consortium (Nakamura, Sasaki, Tagoshi, Tanaka, Poisson) using the Teukolsky formalism for weak perturbations of black holes.[49,50] These small-η calculations have been carried to very high post-Newtonian order for circular orbits and no spins,[51,52] and from those results, Cutler and Flanagan[53] have estimated the order to which the full, finite-η computations must be carried in order that systematic errors in the theoretical templates will not significantly impact the information extracted from the LIGO/VIRGO observational data. The answer appears daunting—radiation-reaction effects must be computed to three full post-Newtonian orders [six orders in $v/c =$(orbital velocity)/(speed of light)] beyond the leading-order radiation reaction, which itself is five orders in v/c beyond the Newtonian theory of gravity.

It is only about ten years since controversies over the leading-order radiation reaction[54] were resolved by a combination of theoretical techniques and binary pulsar observations. Nobody dreamed then that LIGO/VIRGO observations will require pushing post-Newtonian computations onward from $O[(v/c)^5]$ to $O[(v/c)^{11}]$. This requirement epitomizes a major change in the field of relativity research. At last, 80 years after Einstein formulated general relativity, experiment has become a major driver for theoretical analyses.

Remarkably, the goal of $O[(v/c)^{11}]$ is achievable. The most difficult part of the computation, the radiation reaction, has been evaluated to $O[(v/c)^9]$ beyond Newton by the French/Indian/American consortium[48] and as of this writing, rumors have it that $O[(v/c)^{10}]$ is coming under control.

These high-accuracy waveforms are needed only for extracting information from the inspiral waves, after the waves have been discovered; they are not needed for the discovery itself. The discovery is best achieved using a different family of theoretical waveform templates, one that covers the space of potential waveforms in a manner that minimizes computation time instead of a manner that ties quantitatively into general relativity theory.[38] Such templates are in the early stage of development.[55–57]

LIGO/VIRGO observations of compact binary inspirals have the potential to bring us far more information than just binary masses and spins:

- They can be used for high-precision tests of general relativity. In scalar-tensor theories (some of which are attractive alternatives to general relativity[58]), radiation reaction due to emission of scalar waves places a unique signature on the gravitational waves that LIGO/VIRGO would detect—a signature that can be searched for with high precision.[59]

- They can be used to measure the universe's Hubble constant, deceleration parameter, and cosmological constant.[36,37,60,61] The keys to such measurements are that: (1) Advanced interferometers in LIGO/VIRGO will be able to see NS/NS out to cosmological redshifts $z \sim 0.3$ and NS/BH out to $z \sim 2$. (2) The direct observables that can be extracted from the observed waves include the source's luminosity distance $r_{\rm L}$ (measured to accuracy $\sim 10\%$ in a large fraction of cases), and its direction on the sky (to accuracy ~ 1 square degree)—accuracies good enough that only one or a few electromagnetically-observed clusters of galaxies should fall within the three-dimensional gravitational error boxes, thereby giving promise to joint gravitational/electromagnetic statistical studies. (3) Another direct gravitational observable is $(1+z)M$ where z is redshift and M is any mass in the system (measured to the accuracies quoted above). Since the masses of NS's in binaries seem to cluster around $1.4\ M_\odot$, measurements of $(1+z)M$ can provide a handle on the redshift, even in the absence of electromagnetic aid.

- For a NS or small BH spiraling into a massive ~ 50 to $500\ M_\odot$ BH, the inspiral waves will carry a "map" of the spacetime geometry around the big hole—a map that can be used, e.g., to test the theorem that "a black hole has no hair";[62] cf. Sec. 8.3 below.

5.4 Coalescence Waveforms and Their Information

The waves from the binary's final coalescence can bring us new types of information.

BH/BH Coalescence

In the case of a BH/BH binary, the coalescence will excite large-amplitude, highly nonlinear vibrations of spacetime curvature near the coalescing black-hole horizons—a phenomenon of which we have very little theoretical understanding today. Especially fascinating will be the case of two spinning black holes whose spins are not aligned with each other or with the orbital angular momentum. Each of the three angular momentum vectors (two spins, one orbital) will drag space in its vicinity into a tornado-like swirling motion—the general relativistic "dragging of inertial frames," so the binary is rather like two tornados with orientations skewed to each other, embedded inside a third, larger tornado with a third orientation. The dynamical evolution of such a complex configuration of coalescing spacetime warpage (as revealed by its emitted waves) might bring us surprising new insights into relativistic gravity.[14] Moreover, if the sum of the BH masses is fairly large, ~ 40 to $200\ M_\odot$, then the waves should come off in a frequency range $f \sim 40$ to 200 Hz where the LIGO/VIRGO broad-band interferometers have their best sensitivity and can best extract the information the waves carry.

To get full value out of such wave observations will require[63] having theoretical computations with which to compare them. There is no hope to perform such computations analytically; they can only be done as supercomputer simulations. The development of such simulations is being pursued by several research groups, including an eight-university American consortium of numerical relativists and computer scientists called the Two-Black-Holes Grand Challenge Alliance[64] (Co-PIs: Richard Matzner and Jim Browne, University of Texas, Austin; Larry Smarr, Ed Seidel, Paul Saylor, Faisal Saied, University of Illinois, Urbana; Geoffrey Fox, Syracuse University; Stu Shapiro and Saul Teukolsky, Cornell University;

Jim York and Charles Evans, University of North Carolina; Sam Finn, Northwestern University; Pablo Laguna, Pennsylvania State University; and Jeff Winicour, University of Pittsburgh). I have a bet with Matzner, the lead PI of this alliance, that LIGO/VIRGO will discover waves from such coalescences with misaligned spins before the Alliance is able to compute them.

NS/NS Coalescence

The final coalescence of NS/NS binaries should produce waves that are sensitive to the equation of state of nuclear matter, so such coalescences have the potential to teach us about the nuclear equation of state.[14,38] In essence, LIGO/VIRGO will be studying nuclear physics via the collisions of atomic nuclei that have nucleon numbers $A \sim 10^{57}$—somewhat larger than physicists are normally accustomed to. The accelerator used to drive these nuclei up to the speed of light is the binary's self-gravity, and the radiation by which the details of the collisions are probed is gravitational.

Unfortunately, the final NS/NS coalescence will emit its gravitational waves in the kHz frequency band ($800\ \mathrm{Hz} \lesssim f \lesssim 2500\ \mathrm{Hz}$) where photon shot noise will prevent them from being studied by the standard, "workhorse," broad-band interferometers of Fig. 5. However, a specially configured ("dual-recycled") interferometer invented by Brian Meers,[65] which could have enhanced sensitivity in the kHz region at the price of reduced sensitivity elsewhere, may be able to measure the waves and extract their equation of state information, as might massive, spherical, resonant-mass detectors.[38,66] Such measurements will be very difficult and are likely only when the LIGO/VIRGO network has reached a mature stage.

A number of research groups[67–71] are engaged in numerical astrophysics simulations of NS/NS coalescence, with the goal not only to predict the emitted gravitational waveforms and their dependence on equation of state, but also (more immediately) to learn whether such coalescences might power the γ-ray bursts that have been a major astronomical puzzle since their discovery in the early 1970s.

NS/NS coalescence is currently a popular explanation for the γ-ray bursts because (1) the bursts are isotropically distributed on the sky, (2) they have a distribution of number versus intensity that suggests they might lie at near-cosmological distances, and (3) their event rate is roughly the same as that predicted for NS/NS coalescence (~ 1000 per year out to cosmological distances, if they are cosmological). If LIGO/VIRGO were now in operation and observing NS/NS inspiral, it could report definitively whether or not the γ-bursts are produced by NS/NS binaries; and if the answer were yes, then the combination of γ-burst data and gravitational-wave data could bring valuable information that neither could bring by itself. For example, it would reveal when, to within a few msec, the γ-burst is emitted relative to the moment the NS's first begin to touch; and by comparing the γ and gravitational times of arrival, we might test whether gravitational waves propagate with the speed of light to a fractional precision of $\sim 0.01\ \mathrm{sec}/3 \times 10^9\,\mathrm{lyr} = 10^{-19}$.

NS/BH Coalescence

An NS spiraling into a BH of mass $M \gtrsim 10\ M_\odot$ should be swallowed more or less whole. However, if the BH is less massive than roughly 10 $M_\odot$, and especially if it is rapidly rotating, then the NS will tidally disrupt before being swallowed. Little is known about the disruption and accompanying waveforms. To model them with any reliability will likely require full numerical relativity, since the circumferences of the BH and NS will be comparable and their physical separation at the moment of disruption will be of the same order as their separation. As with NS/NS, the coalescence waves should carry equation of state information and will come out in the kHz band, where their detection will require advanced, specialty detectors.

Christodoulou Memory

As the coalescence waves depart from their source, their energy creates (via the nonlinearity of Einstein's field equations) a secondary wave called the "Christodoulou memory."[72–74] Whereas the primary waves may have frequencies in the kHz band, the memory builds up on the timescale of the primary energy emission profile, which is likely to be of order 0.01 sec, corresponding to a memory frequency in the optimal band for the LIGO/VIRGO workhorse interferometers, $\sim$ 100 Hz. Unfortunately, the memory is so weak that only very advanced interferometers have much chance of detecting and studying it—and then, perhaps only for BH/BH coalescences and not for NS/NS or NS/BH.[75]

6 Other High-Frequency Sources

6.1 Stellar Core Collapse and Supernovae

When the core of a massive star has exhausted its supply of nuclear fuel, it collapses to form a neutron star or black hole. In some cases, the collapse triggers and powers a subsequent explosion of the star's mantle—a supernova explosion. Despite extensive theoretical efforts for more than 30 years, and despite wonderful observational data from Supernova 1987A, theorists are still far from a definitive understanding of the details of the collapse and explosion. The details are highly complex and may differ greatly from one core collapse to another.[76]

Several features of the collapse and the core's subsequent evolution can produce significant gravitational radiation in the high-frequency band. We shall consider these features in turn, the most weakly radiating first.

Boiling of the Newborn Neutron Star

Even if the collapse is spherical, so it cannot radiate any gravitational waves at all, it should produce a convectively unstable neutron star that "boils" vigorously (and nonspherically) for the first ~ 0.1 second of its life.[77] The boiling dredges up high-temperature nuclear matter ($T \sim 10^{12}$ K) from the neutron star's central regions, bringing it to the surface (to the "neutrino-sphere"), where it cools by neutrino emission before being swept back downward and reheated. Burrows estimates[78,79] that the boiling should generate $n \sim 10$ cycles of gravitational waves with frequency $f \sim 100$ Hz and amplitude $h \sim 3 \times 10^{-22}(30 \text{ kpc}/r)$ (where r is the distance to the source), corresponding to a characteristic amplitude $h_c \simeq h\sqrt{n} \sim 10^{-21}(30 \text{ kpc}/r)$, cf. Fig. 12. LIGO/VIRGO will be able to detect such waves only in the local group of galaxies, where the supernova rate is probably no larger than ~ 1 every ten years. However, neutrino detectors have a similar range, and there could be a high scientific payoff from correlated observations of the gravitational waves emitted by the boiling's mass motions and neutrinos emitted from the boiling neutrino-sphere.

Axisymmetric Collapse, Bounce, and Oscillations

Rotation will centrifugally flatten the collapsing core, enabling it to radiate as it implodes. If the core's angular momentum is small enough that centrifugal forces do not halt or strongly slow the collapse before it reaches nuclear densities, then

Figure 12: Characteristic amplitudes of the gravitational waves from various processes accompanying stellar core collapse and supernovae, compared with projected sensitivities of LIGO's interferometers.

the core's collapse, bounce, and subsequent oscillations are likely to be axially symmetric. Numerical simulations[80,81] show that in this case, the waves from collapse, bounce, and oscillation will be quite weak: the total energy radiated as gravitational waves is not likely to exceed $\sim 10^{-7}$ solar masses (about one part in a million of the collapse energy) and might often be much less than this; and correspondingly, the waves' characteristic amplitude will be $h_c \lesssim 3 \times 10^{-21}(30\ \mathrm{kpc}/r)$. These collapse-and-bounce waves will come off at frequencies ~ 200 Hz to ~ 1000 Hz and will precede the boiling waves by a fraction of a second. Like the boiling waves, they probably cannot be seen by LIGO/VIRGO beyond the local group of galaxies and thus will be a very rare occurrence.

Rotation-Induced Bars and Break-Up

If the core's rotation is large enough to strongly flatten the core before or as it reaches nuclear density, then a dynamical and/or secular instability is likely to break the core's axisymmetry. The core will be transformed into a bar-like configuration that spins end-over-end like an American football, and that might even break up into two or more massive pieces. In this case, the radiation from the spinning bar or orbiting pieces *could* be almost as strong as that from a coalescing neutron-star binary, and thus, could be seen by the LIGO/VIRGO first interferometers out to the distance of the Virgo cluster (where the supernova rate is several per year) and by advanced interferometers out to several hundred Mpc (supernova rate $\sim 10^4$ per year), cf. Fig. 12. It is far from clear what fraction of collapsing cores will have enough angular momentum to break their axisymmetry, and what fraction of those will actually radiate at this high rate; but even if only $\sim 1/1000$ or $1/10^4$ do so, this could ultimately be a very interesting source for LIGO/VIRGO.

Several specific scenarios for such nonaxisymmetry have been identified:

Centrifugal hangup at $\sim$ 100 km radius: If the precollapse core is rapidly spinning (e.g., if it is a white dwarf that has been spun up by accretion from a companion), then the collapse may produce a highly flattened, centrifugally supported disk with most of its mass at radii $R \sim 100$ km, which then (via instability) may transform itself into a bar or may bifurcate. The bar or bifurcated lumps will radiate gravitational waves at twice their rotation frequency, $f \sim 100$ Hz—the optimal frequency for LIGO/VIRGO interferometers. To shrink on down to ~ 10 km size, this configuration must shed most of its angular momentum. *If* a substantial fraction of the angular momentum goes into gravitational waves, then independently of the strength of the bar, the waves will be nearly as strong as those from a coalescing binary. The reason is the waves' amplitude h is proportional to the bar's ellipticity e, the number of cycles n of wave emission is proportional to $1/e^2$, and the characteristic amplitude $h_c = h\sqrt{n}$ is thus independent of the ellipticity and is about the same whether the configuration is a bar or is two lumps.[37] The resulting waves will thus have h_c roughly half as large, at $f \sim 100$ Hz, as the h_c from a NS/NS binary (half as large because each lump might be half as massive as a NS), and the waves will chirp upward in frequency in a manner similar to those from a binary.

It is rather likely, however, that most of excess angular momentum does *not* go into gravitational waves, but instead, goes largely into hydrodynamic waves as the bar or lumps, acting like a propeller to stir up the surrounding stellar mantle. In this case, the radiation will be correspondingly weaker.

Centrifugal hangup at $\sim$ 20 km radius: Lai and Shapiro[82] have explored the case of centrifugal hangup at radii not much larger than the final neutron star, say $R \sim 20$ km. Using compressible ellipsoidal models, they have deduced that, after a brief period of dynamical bar-mode instability with wave emission at

$f \sim 1000$ Hz (explored by Houser, Centrella, and Smith[83]), the star switches to a secular instability in which the bar's angular velocity gradually slows while the material of which it is made retains its high rotation speed and circulates through the slowing bar. The slowing bar emits waves that sweep *downward* in frequency through the LIGO/VIRGO optimal band $f \sim 100$ Hz, toward ~ 10 Hz. The characteristic amplitude (Fig. 12) is only modestly smaller than for the upward-sweeping waves from hangup at $R \sim 100$ km, and thus, such waves should be detectable near the Virgo Cluster by the first LIGO/VIRGO interferometers, and at distances of a few 100 Mpc by advanced interferometers.

Successive fragmentations of an accreting, newborn neutron star: Bonnell and Pringle[84] have focused on the evolution of the rapidly spinning, newborn neutron star as it quickly accretes more and more mass from the presupernova star's inner mantle. If the accreting material carries high angular momentum, it may trigger a renewed bar formation, lump formation, wave emission, and coalescence, followed by more accretion, bar and lump formation, wave emission, and coalescence. Bonnell and Pringle speculate that hydrodynamics, not wave emission, will drive this evolution, but that the total energy going into gravitational waves might be as large as $\sim 10^{-3}\, M_\odot$. This corresponds to $h_c \sim 10^{-21}(10\ \mathrm{Mpc}/r)$.

6.2 Spinning Neutron Stars; Pulsars

As the neutron star settles down into its final state, its crust begins to solidify (crystalize). The solid crust will assume nearly the oblate axisymmetric shape that centrifugal forces are trying to maintain, with poloidal ellipticity $\epsilon_p \propto$ (angular velocity of rotation).[2] However, the principal axis of the star's moment of inertia tensor may deviate from its spin axis by some small "wobble angle" θ_w, and the star may deviate slightly from axisymmetry about its principal axis; i.e., it may have a slight ellipticity $\epsilon_e \ll \epsilon_p$ in its equatorial plane.

As this slightly imperfect crust spins, it will radiate gravitational waves:[85] ϵ_e radiates at twice the rotation frequency, $f = 2\, f_{\rm rot}$ with $h \propto \epsilon_e$, and the wobble angle couples to ϵ_p to produce waves at $f = f_{\rm rot} + f_{\rm prec}$ (the precessional sideband of the rotation frequency) with amplitude $h \propto \theta_w \epsilon_p$. For typical neutron-star masses and moments of inertia, the wave amplitudes are

$$h \sim 6 \times 10^{-25} \left(\frac{f_{\rm rot}}{500\ \mathrm{Hz}}\right)^2 \left(\frac{1\ \mathrm{kpc}}{r}\right) \left(\frac{\epsilon_e \text{ or } \theta_w \epsilon_p}{10^{-6}}\right) . \qquad (5)$$

The neutron star gradually spins down, due in part to gravitational-wave emission, but perhaps more strongly due to electromagnetic torques associated with its spinning magnetic field and pulsar emission. This spin-down reduces the strength of centrifugal forces and thereby causes the star's poloidal ellipticity ϵ_p to decrease, with an accompanying breakage and resolidification of its crust's crystal structure (a "starquake").[86] In each starquake, θ_w, ϵ_e, and ϵ_p will all change suddenly, thereby changing the amplitudes and frequencies of the star's two gravitational "spectral lines" $f = 2\, f_{\rm rot}$ and $f = f_{\rm rot} + f_{\rm prec}$. After each quake, there should be a healing period in which the star's fluid core and solid crust, now rotating at different speeds, gradually regain synchronism. By monitoring the amplitudes, frequencies, and phases of the two gravitational-wave spectral lines, and by comparing with timing of the electromagnetic pulsar emission, one might learn much about the physics of the neutron-star interior.

How large will the quantities ϵ_e and $\theta_w \epsilon_p$ be? Rough estimates of the crustal shear moduli and breaking strengths suggest an upper limit in the range $\epsilon_{\rm max} \sim 10^{-4}$ to 10^{-6}, and it might be that typical values are far below this. We are extremely ignorant, and correspondingly, there is much to be learned from searches for gravitational waves from spinning neutron stars.

One can estimate the sensitivity of LIGO/VIRGO (or any other broad-band detector) to the periodic waves from such a source by multiplying the waves' amplitude h by the square root of the number of cycles over which one might integrate to find the signal, $n = f\hat{\tau}$ where $\hat{\tau}$ is the integration time. The resulting effective signal strength, $h\sqrt{n}$, is larger than h by

$$\sqrt{n} = \sqrt{f\hat{\tau}} = 10^5 \left(\frac{f}{1000\ {\rm Hz}}\right)^{1/2} \left(\frac{\hat{\tau}}{4\ {\rm months}}\right)^{1/2} . \qquad (6)$$

This $h\sqrt{n}$ should be compared (1) to the detector's rms broad-band noise level for sources in a random direction, $\sqrt{5}h_{\rm rms}$, to deduce a signal-to-noise ratio, or (2) to $h_{\rm SB}$ to deduce a sensitivity for high-confidence detection when one does not know the waves' frequency in advance.[6] Such a comparison suggests that the first interferometers in LIGO/VIRGO might possibly see waves from nearby spinning neutron stars, but the odds of success are very unclear.

The deepest searches for these nearly periodic waves will be performed by narrow-band detectors, whose sensitivities are enhanced near some chosen frequency at the price of sensitivity loss elsewhere—e.g., dual-recycled interferometers[65] or resonant-mass antennas (Sec. 4). With "advanced-detector technology," dual-recycled interferometers might be able to detect with confidence all spinning neutron stars that have[6]

$$(\epsilon_e \text{ or } \theta_w \epsilon_p) \gtrsim 3 \times 10^{-10} \left(\frac{500 \text{ Hz}}{f_{\rm rot}} \right)^2 \left(\frac{r}{1000 \text{ pc}} \right)^2 . \tag{7}$$

There may well be a large number of such neutron stars in our galaxy; but it is also conceivable that there are none. We are extremely ignorant.

Some cause for optimism arises from several physical mechanisms that might generate radiating ellipticities large compared to 3×10^{-10}:

- It may be that, inside the superconducting cores of many neutron stars, there are trapped magnetic fields with mean strength $B_{\rm core} \sim 10^{13}$ G or even 10^{15} G. Because such a field is actually concentrated in flux tubes with $B = B_{\rm crit} \sim 6 \times 10^{14}$ G surrounded by a field-free superconductor, its mean pressure is $p_B = B_{\rm core} B_{\rm crit}/8\pi$. This pressure could produce a radiating ellipticity $\epsilon_{\rm e} \sim \theta_w \epsilon_p \sim p_B/p \sim 10^{-8} B_{\rm core}/10^{13}$ G (where p is the core's material pressure).
- Accretion onto a spinning neutron star can drive precession (keeping θ_w substantially nonzero), and thereby might produce measurably strong waves.[87]
- If a neutron star is born rotating very rapidly, then it may experience a gravitational-radiation-reaction-driven instability. In this "CFS" (Chandrasekhar,[88] Friedman, Schutz[89]) instability, density waves propagate around the star in the opposite direction to its rotation, but are dragged forward by the rotation. These density waves produce gravitational waves that carry positive energy as seen by observers far from the star, but negative energy from the star's viewpoint; and because the star thinks it is losing negative energy, its density waves get amplified. This intriguing mechanism is similar to that by which spiral density waves are produced in galaxies. Although the CFS instability was once thought ubiquitous for spinning stars,[89,90] we now know that neutron-star viscosity will kill it, stabilizing the star and turning off the waves, when the star's temperature is above some limit $\sim 10^{10}$ K (Ref. 91) and below some limit $\sim 10^9$K (Ref. 92); and correspondingly, the instability should operate only during the first few years of a neutron star's life, when $10^9 \text{ K} \lesssim T \lesssim 10^{10}$ K.

6.3 Stochastic Background

There should be a stochastic background of gravitational waves in the high-frequency band produced by processes in the early universe. Because this background will extend over all gravitational-wave frequencies, not just high frequencies, we shall delay discussing it until Sec. 9.

7 LISA: The Laser Interferometer Space Antenna

Turn now, from the high-frequency band, 1–10^4 Hz, to the low-frequency band, 10^{-4}–1 Hz. At present, the most sensitive gravitational-wave searches at low frequencies are those carried out by researchers at NASA's Jet Propulsion Laboratory, using microwave-frequency Doppler tracking of interplanetary spacecraft. These searches are done at rather low cost, piggy-backing missions designed for other purposes. Although they have a possibility of success, the odds are against them. Their best past sensitivities to bursts, for example, have been $h_{\rm SB} \sim 10^{-14}$, and prospects are good for reaching $\sim 10^{-15}$–10^{-16} in the next five to ten years. However, the strongest low-frequency bursts arriving several times per year might be no larger than $\sim 10^{-18}$; and the domain of an assured plethora of signals is $h_{\rm SB} \sim 10^{-19}$–10^{-20}.

To reach into this assured-detection domain will almost certainly require switching from microwave-frequency tracking of spacecraft (with its large noise due to fluctuating dispersion in the troposphere and interplanetary plasma) to optical tracking. Such a switch is planned for the 2014 time frame or sooner, when the European Space Agency (ESA) and/or NASA is likely to fly the *Laser Interferometer Space Antenna*, LISA.

7.1 Mission Status

LISA is largely an outgrowth of 15 years of studies by Peter Bender and colleagues at the University of Colorado. In 1990, NASA's Ad Hoc Committee on Gravitation Physics and Astronomy selected a LISA-type gravitational-wave detector as its highest priority in the large space mission category;[93] and since then, enthusiasm for LISA has continued to grow within the American gravitation community.

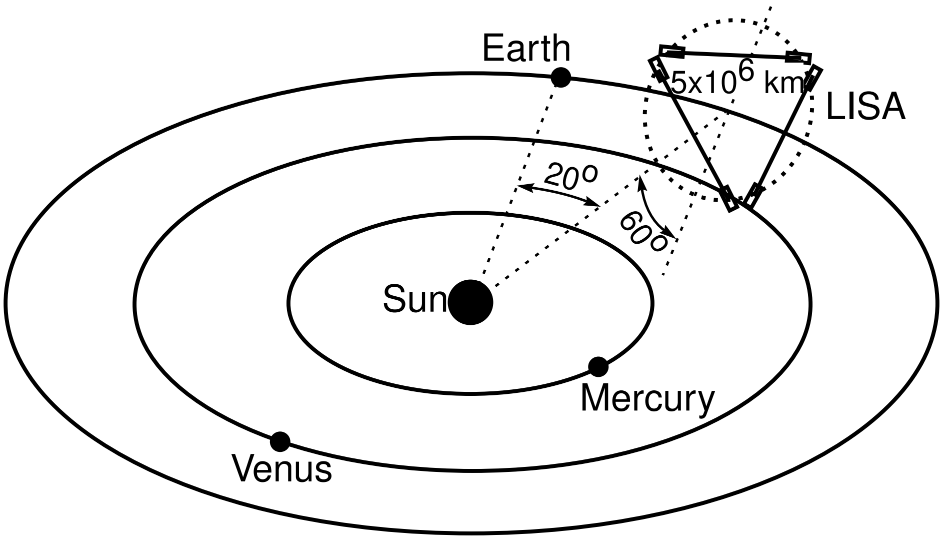

Figure 13: LISA's orbital configuration, with LISA magnified in arm length by a factor ~ 10 relative to the solar system.

Unfortunately, the prospects for NASA to fly such a mission did not look good in the early 1990s. By contrast, prospects in Europe looked much better, so a largely European consortium was put together in 1993, under the leadership of Karsten Danzmann (Hannover) and James Hough (Glasgow), to propose LISA to the ESA. This proposal has met with considerable success; LISA might well achieve approval to fly as an ESA Cornerstone Mission around 2014.[94] Members of the American gravitation community and members of the LISA team hope that NASA will join together with ESA in this endeavor, and that working jointly, ESA and NASA will be able to fly LISA considerably sooner than 2014.

7.2 Mission Configuration

As presently conceived, LISA will consist of six compact, drag-free spacecrafts (i.e., spacecrafts that are shielded from buffeting by solar wind and radiation pressure) which therefore move very nearly on geodesics of spacetime. All six spacecrafts would be launched simultaneously by a single Ariane rocket. They would be placed into the same heliocentric orbit as the Earth occupies but would follow 20° behind the Earth; cf. Fig. 13. The spacecrafts would fly in pairs, with each pair at the vertex of an equilateral triangle that is inclined at an angle of 60° to the Earth's orbital plane. The triangle's arm length would be 5 million km

(10^6 times larger than LIGO's arms!). The six spacecrafts would track each other optically, using one-Watt YAG laser beams. Because of diffraction losses over the 5×10^6 km arm length, it is not feasible to reflect the beams back and forth between mirrors as is done with LIGO. Instead, each spacecraft will have its own laser; and the lasers will be phase locked to each other, thereby achieving the same kind of phase-coherent out-and-back light travel as LIGO achieves with mirrors. The six-laser, six-spacecraft configuration thereby functions as three, partially-independent, but partially-redundant, gravitational-wave interferometers.

7.3 Noise and Sensitivity

Figure 14 depicts the expected noise and sensitivity of LISA in the same language as we have used for LIGO (Fig. 5). The curve at the bottom of the stippled region is $h_{\rm rms}$, the rms noise, in a bandwidth equal to frequency, for waves with optimum direction and polarization. The top of the stippled region is $h_{\rm SB} = 5\sqrt{5}\ h_{\rm rms}$, the sensitivity for high-confidence detection ($S/N = 5$) of a broad-band burst coming from a random direction, assuming Gaussian noise.

At frequencies $f \gtrsim 10^{-3}$ Hz, LISA's noise is due to photon counting statistics (shot noise). The noise curve steepens at $f \sim 3 \times 10^{-2}$ Hz because at lower frequencies the waves' period is longer than the round-trip light travel time in one of LISA's arms. Below 10^{-3} Hz, the noise is due to buffeting-induced random motions of the spacecraft that are not being properly removed by the drag-compensation system. Notice that, in terms of dimensionless amplitude, LISA's sensitivity is roughly the same as that of LIGO's first interferometers (Fig. 9), but at 100,000 times lower frequency. Since the waves' energy flux scales as f^2h^2, this corresponds to 10^{10} better energy sensitivity than LIGO.

7.4 Observational Strategy

LISA can detect and study, simultaneously, a wide variety of different sources scattered over all directions on the sky. The key to distinguishing the different sources is the different time evolution of their waveforms. The key to determining each source's direction, and confirming that it is real and not just noise, is the manner in which its waves' amplitude and frequency are modulated by LISA's complicated orbital motion—a motion in which the interferometer triangle rotates

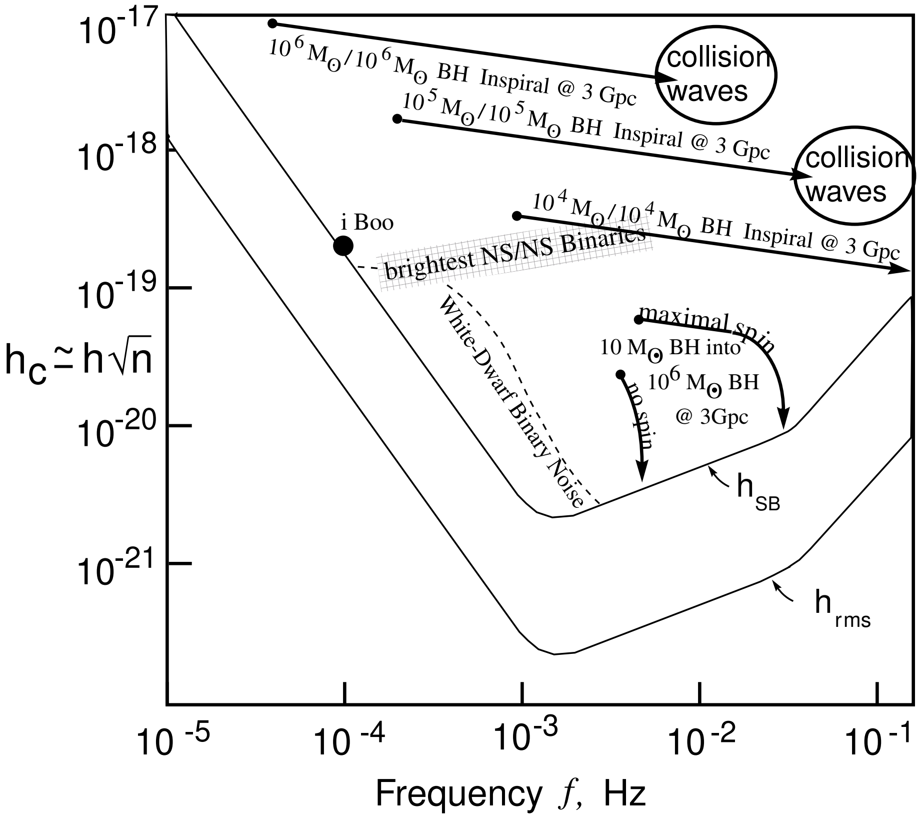

Figure 14: LISA's projected broad-band noise $h_{\rm rms}$ and sensitivity to bursts $h_{\rm SB}$, compared with the strengths of the waves from several low-frequency sources. [*Note:* When members of the LISA team plot curves analogous to this, they show the sensitivity curve (top of stippled region) in units of the amplitude of a periodic signal that can be detected with $S/N = 5$ in one year of integration; that sensitivity to periodic sources is related to the $h_{\rm SB}$ used here by $h_{\rm SP} = h_{\rm SB}/\sqrt{f \cdot 3 \times 10^7 {\rm sec}}$.]

around its center once per year, and the interferometer plane precesses around the normal to the Earth's orbit once per year. Most sources will be observed for a year or longer, thereby making full use of these modulations.

8 Low-Frequency Gravitational-Wave Sources

8.1 Waves from Binary Stars

LISA has a large class of guaranteed sources—short-period binary stars in our own galaxy. A specific example is the classic binary 44 i Boo (HD133640), a 1.35 $M_\odot/0.68\ M_\odot$ system just 12 parsecs from Earth, whose wave frequency f and characteristic amplitude $h_c = h\sqrt{n}$ are depicted in Fig. 14. (Here, h is the waves' actual amplitude and $n = f\hat{\tau}$ is the number of wave cycles during $\hat{\tau} = 1$ year of signal integration). Since 44 i Boo lies right on the $h_{\rm SB}$ curve, its signal-to-noise ratio in one year of integration should be $S/N = 5$.

To have an especially short period, a binary must be made of especially compact bodies—white dwarfs (WD), neutron stars (NS), and/or black holes (BH). WD/WD binaries are thought to be so numerous that they may produce a stochastic background of gravitational waves, at the level shown in Fig. 14, that will hide some other interesting waves from view.[95] Since WD/WD binaries are very dim optically, their actual numbers are not known for sure; Fig. 14 might be an overestimate.

Assuming a NS/NS coalescence rate of one each 10^5 years in our galaxy,[27,28] the shortest period NS/NS binary should have a remaining life of about 5×10^4 years, corresponding to a gravitational-wave frequency today of $f \simeq 5 \times 10^{-3}$ Hz, an amplitude (at about 10 kpc distance) $h \simeq 4 \times 10^{-22}$, and a characteristic amplitude (with one year of integration time) $h_c \simeq 2 \times 10^{-19}$. This is depicted in Fig. 14 at the right edge of the region marked "brightest NS/NS binaries." These brightest NS/NS binaries can be studied by LISA with the impressive signal-to-noise ratios $S/N \sim 50$ to 500.

8.2 Waves from the Coalescence of Massive Black Holes in Distant Galaxies

LISA would be a powerful instrument for studying massive black holes in distant galaxies. Figure 14 shows, as examples, the waves from several massive black hole binaries at a 3 Gpc distance from Earth (a cosmological redshift of unity). The waves sweep upward in frequency (rightward in the diagram) as the holes spiral together. The black dots show the waves' frequency one year before the holes' final collision and coalescence, and the arrowed lines show the sweep of frequency and characteristic amplitude $h_c = h\sqrt{n}$ during that last year. For simplicity, the figure is restricted to binaries with equal-mass black holes: $10^4\ M_\odot/10^4\ M_\odot$, $10^5\ M_\odot/10^5\ M_\odot$, and $10^6\ M_\odot/10^6\ M_\odot$.

By extrapolation from these three examples, we see that LISA can study much of the last year of inspiral, and the waves from the final collision and coalescence, whenever the holes' masses are in the range $3 \times 10^4\ M_\odot \lesssim M \lesssim 10^8\ M_\odot$. Moreover, LISA can study the final coalescences with remarkable signal to noise ratios: $S/N \gtrsim 1000$. Since these are much larger S/N's than LIGO/VIRGO is likely to achieve, we can expect LISA to refine the experimental understanding of black-hole physics and of highly nonlinear vibrations of warped spacetime, which LIGO/VIRGO initiates—*provided* the rate of massive black-hole coalescences is of order of one per year in the Universe or higher. The rate might well be that high, but it also might be much lower.

By extrapolating Fig. 14 to lower BH/BH masses, we see that LISA can observe the last few years of inspiral, but not the final collisions, of binary black holes in the range $100\ M_\odot \lesssim M \lesssim 10^4\ M_\odot$, out to cosmological distances.

Extrapolating the BH/BH curves to lower frequencies using the formula (time to final coalescence) $\propto f^{-8/3}$, we see that equal-mass BH/BH binaries enter LISA's frequency band roughly 1000 years before their final coalescences, more or less independently of their masses, for the range $100\ M_\odot \lesssim M \lesssim 10^6\ M_\odot$. Thus, if the coalescence rate were to turn out to be one per year, LISA would see roughly 1000 additional massive binaries that are slowly spiraling inward, with inspiral rates df/dt readily measurable. From the inspiral rates, the amplitudes of the two polarizations, and the waves' harmonic content, LISA can determine each such binary's luminosity distance, redshifted chirp mass $(1+z)\ M_c$, orbital inclination, and eccentricity; and from the waves' modulation by LISA's orbital motion, LISA can learn the direction to the binary with an accuracy of order of one degree.

8.3 Waves from Compact Bodies Spiraling into Massive Black Holes in Distant Galaxies

When a compact body with mass μ spirals into a much more massive black hole with mass M, the body's orbital energy E at fixed frequency f (and correspondingly at fixed orbital radius a) scales as $E \propto \mu$, the gravitational-wave luminosity $\dot{E}$ scales as $\dot{E} \propto \mu^2$, and the time to final coalescence thus scales as $t \sim E/\dot{E} \propto 1/\mu$. This means that the smaller is μ/M, the more orbits are spent in the hole's strong-gravity region, $a \lesssim 10\ GM/c^2$, and thus, the more detailed and accurate will be the map of the hole's spacetime geometry, which is encoded in the emitted waves.

For holes observed by LIGO/VIRGO, the most extreme mass ratio that we can hope for is $\mu/M \sim 1\ M_\odot/300\ M_\odot$, since for $M > 300\ M_\odot$, the inspiral waves are pushed to frequencies below the LIGO/VIRGO band. This limit on μ/M seriously constrains the accuracy with which LIGO/VIRGO can hope to map out the spacetime geometries of black holes and test the black-hole no-hair theorem[62] (end of Sec. 5.3). By contrast, LISA can observe the final inspiral waves from objects of any mass $M \gtrsim 0.5\ M_\odot$ spiraling into holes of mass $3 \times 10^5\ M_\odot \lesssim M \lesssim 3 \times 10^7\ M_\odot$.

Figure 14 shows the example of a 10 $M_\odot$ black hole spiraling into a $10^6\ M_\odot$ hole at a 3 Gpc distance. The inspiral orbit and waves are strongly influenced by the hole's spin. Two cases are shown:[96] an inspiraling circular orbit around a nonspinning hole, and a prograde, circular, equatorial orbit around a maximally spinning hole. In each case, the dot at the upper left end of the arrowed curve is the frequency and characteristic amplitude one year before the final coalescence. In the nonspinning case, the small hole spends its last year spiraling inward from $r \simeq 7.4\ GM/c^2$ (3.7 Schwarzschild radii) to its last stable circular orbit at $r = 6\ GM/c^2$ (3 Schwarzschild radii). In the maximal spin case, the last year is spent traveling from $r = 6\ GM/c^2$ (3 Schwarzschild radii) to the last stable orbit at $r = GM/c^2$ (half a Schwarzschild radius). The $\sim 10^5$ cycles of waves during this last year should carry, encoded in themselves, rather accurate values for the massive hole's lowest few multipole moments.[97] If the measured moments satisfy the "no-hair" theorem (i.e., if they are all determined uniquely by the measured mass and spin in the manner of the Kerr metric), then we can be sure the central body is a black hole. If they violate the no-hair theorem, then (assuming general relativity is correct), either the central body was not a black hole, or an accretion disk or other material was perturbing its orbit.[98] From the evolution of the waves, one can hope to determine which is the case and to explore the properties of the central body and its environment.[62]

Models of galactic nuclei, where massive holes reside, suggest that inspiraling stars and small holes typically will be in rather eccentric orbits.[99] This is because they get injected into such orbits via gravitational deflections off other stars, and by the time gravitational radiation reaction becomes the dominant orbital driving force, there is not enough inspiral left to fully circularize their orbits. Such orbital eccentricity will complicate the waveforms and complicate the extraction of information from them. Efforts to understand the emitted waveforms are just now getting underway.

The event rates for inspiral into massive black holes are not at all well understood. However, since a significant fraction of all galactic nuclei are thought to contain massive holes, and since white dwarfs and neutron stars, as well as small black holes, can withstand tidal disruption as they plunge toward the massive hole's horizon, and since LISA can see inspiraling bodies as small as $\sim 0.5\ M_\odot$ out to a 3 Gpc distance, the event rate is likely to be interestingly large.

9 The Stochastic Gravitational-Wave Background

Processes in the early universe should have produced a stochastic background of gravitational waves that extends through the entire frequency range from extremely low frequencies $f \sim 10^{-18}$ Hz to the high-frequency band $f \sim 1$—10^4 Hz and beyond.

9.1 Primordial Gravitational Waves

The most interesting background would be that produced in the Big Bang itself. Zel'dovich and Novikov have estimated[100] that the optical thickness of primordial matter to gravitational waves has been small compared to unity at all times since the Planck era, when space and time came into being, and that therefore, primordial gravitational waves (by contrast with electromagnetic) should not have been thermalized by interactions with matter. On the other hand (as Grishchuk has shown[101]), whatever might have been the state of the graviton field when it emerged from the Big Bang's Planck era, it should have interacted with the subsequent, early-time expansion of the universe to produce, via parametric amplification, a rich spectrum of stochastic waves today. The details of that spectrum depend on what emerged from the Planck era and on the evolution $a(t)$ of the universal expansion factor at early times.

The gravitational-wave spectrum is generally described by the quantity $\Omega_g(f) =$ (energy density in a bandwidth equal to frequency f)/(energy density required to close the universe); cf. Sec. 2.3. The observed quadrupolar anisotropy of the cosmic microwave radiation places a limit $\Omega_g \lesssim 10^{-9}$ at $f \sim 10^{-18}$ Hz (Sec. 2.4). It is fashionable to extrapolate this limit to higher frequencies by *assuming* that the graviton field emerged from the Planck era in its vacuum state and *assuming* that the universal expansion $a(t)$ was that of an inflationary era $a \propto e^{Ht}$ for some constant H, followed by a radiation-dominated Friedman era $a \propto t^{1/2}$, followed by the present matter-dominated era $a \propto t^{2/3}$. This standard model produces a flat spectrum Ω_g independent of f for all waves that entered our cosmological horizon during the radiation-dominated era, which means at all frequencies from $\sim 10^{-16}$ Hz up through the high-frequency band and somewhat beyond. The observational limit at 10^{-18} Hz implies that this constant value is $\Omega_g \lesssim 3 \times 10^{-14}$ (Refs. 12 and 102). So a weak background cannot be detected by LIGO in the high-frequency band, nor by LISA at low frequencies, nor by pulsar timing at very low frequencies. LIGO's limiting sensitivities will correspond to $\Omega_g \sim$ (a few) $\times 10^{-7}$ at $f \sim 10^{2}$ Hz for the first interferometers, and $\Omega_g \sim$ (a few) $\times 10^{-10}$ for advanced interferometers;[103] LISA's sensitivity will correspond to $\Omega_g \sim$ (a few) $\times 10^{-10}$ at $f \sim 10^{-3}$ Hz; and the present pulsar timing measurements correspond to $\Omega_g \sim$ (a few) $\times 10^{-8}$ at $f \sim 4 \times 10^{-9}$ Hz (Sec. 2.3 and Ref. 9).

On the other hand, if the graviton field did not begin in its vacuum state, or if the equation of state in the very early Friedman era was stiffer than that of radiation, then the primordial backgrounds at high, low, and very low frequencies could be significantly stronger than $\Omega \sim 3 \times 10^{-14}$ and could be strong enough to detect.

9.2 Waves from Phase Transitions in the Early Universe

A stochastic background could also have been produced by phase transitions in the early universe.[104,105] No known phase transition would put its waves into the high-frequency band, and even hypothetical phase transitions, optimized at high-frequencies, can be only strong enough for marginal detection by advanced LIGO interferometers. The prospects for LISA are a little better. A strongly first-order electroweak phase transition could produce low-frequency waves strong enough for LISA to detect.[105]

9.3 Waves from Cosmic Strings

If cosmic strings[106] were produced in the early universe in as large numbers as some theorists have suggested,[10,11] their vibrations would produce a gravitational wave spectrum that is frequency independent, $\Omega_g = \text{const}$, from below the very-low-frequency band where pulsar timing operates, through LISA's low-frequency band, and on into and through the high-frequency band. Theory suggests[107] that such waves could be as strong as $\Omega_g \sim 10^{-7}$—a level that is already being constrained by pulsar timing observations (Sec. 2.3). LIGO's first interferometers will operate at this same level, and by the time LIGO's advanced interferometers and LISA reach $\Omega_g \sim$ (a few) $\times 10^{-10}$, pulsar timing might be in that same range.

To summarize: there are known mechanisms that could easily produce a measurable stochastic background in the high-, low-, and very-low-frequency bands. However, the odds of the background being that large, based on currently fashionable ideas, are not great. Despite this, a vigorous effort to detect background waves and to map their spectrum will surely be made, since the cosmological implications of their discovery could be profound.

10 Conclusion

It is now 35 years since Joseph Weber initiated his pioneering development of gravitational-wave detectors[23] and 25 years since Forward[108] and Weiss[16] initiated work on interferometric detectors. Since then, hundreds of talented experimental physicists have struggled to improve the sensitivities of these instruments. At last, success is in sight. If the source estimates described in this review article are approximately correct, then the planned interferometers should detect the first waves in 2001 or several years thereafter, thereby opening up this rich new window onto the universe.

11 Acknowledgments

For insights into the rates of coalescence of compact binaries, I thank Sterl Phinney. My group's research on gravitational waves and their relevance to LIGO/ VIRGO and LISA is supported in part by NSF grants AST-9417371 and PHY-9424337, and by NASA grant NAGW-4268. Portions of this article were adapted from my Ref. 109.

References

[1] A. Pais, *'Subtle is the Lord...' The Science and the Life of Albert Einstein.* (Clarendon Press, Oxford, 1982).

[2] R. A. Hulse and J. H. Taylor, Astrophys. J. **324**, 355 (1975).

[3] J. H. Taylor, Rev. Mod. Phys. **66**, 711 (1994).

[4] C. M. Will, *Theory and Experiment in Gravitational Physics.* (Cambridge University Press, 1994).

[5] T. Damour and J. Taylor, Phys. Rev. D **45**, 1840 (1992).

[6] K. S. Thorne, in *Three Hundred Years of Gravitation*, edited by S. W. Hawking and W. Israel (Cambridge University Press, 1987), pp. 330-458.

[7] K. S. Thorne, in *Gravitational Radiation*, edited by N. Deruelle and T. Piran, (North Holland, 1983), p. 1.

[8] W. J. Sullivan, *The Early Years of Radio Astronomy.* (Cambridge University Press, 1984).

[9] V. M. Kaspi, J. H. Taylor, and M. F. Ryba, Astrophys. J. **428**, 713 (1994).

[10] Y. B. Zel'dovich, Mon. Not. R. Astron. Soc. **192**, 663 (1980).

[11] A. Vilenkin, Phys. Rev. D **24**, 2082 (1981).

[12] L. M. Krauss and M. White, Phys. Rev. Lett. **69**, 969 (1992).

[13] R. L. Davis, H. M. Hodges, G. F. Smoot, P. J. Steinhardt, and M. S. Turner, Phys. Rev. Lett. **69**, 1856 (1992).

[14] A. Abramovici *et. al.*, Science **256**, 325 (1992).

[15] R. W. P. Drever, in *Gravitational Radiation*, edited by N. Deruelle and T. Piran (North Holland, 1983), p. 321 and references therein.

[16] R. Weiss, *Quarterly Progress Report of RLE, MIT*, **105**, 54 (1972).

[17] C. Bradaschia *et. al.*, Nucl. Instrum. Methods A **289**, 518 (1990).

[18] S. E. Whitcomb and the LIGO R&D science team, LIGO Report Number 94-7, November 1994.

[19] P. Saulson, Phys. Rev. D **42**, 2437 (1990).

[20] V. B. Braginsky, V. P. Mitrofanov, and O. A. Okhrimenko, Phys. Lett. A **175**, 82 (1993).

[21] A. Gillespie and F. Raab, Phys. Lett. A **190**, 213 (1994).

[22] W. W. Johnson and S. M. Merkowitz, Phys. Rev. Lett. **70**, 2367 (1993).

[23] J. Weber, Phys. Rev. **117**, 306 (1960).

[24] M. Bassan, Class. Quant. Grav. **11**, Supplement: A39 (1994).

[25] G. Pizella, Nucl. Phys. B, Supplement: 28A, 48 (1992).

[26] J. Hough and K. Danzmann *et. al*, GEO600, Proposal for a 600 m Laser-Interferometric Gravitational Wave Antenna, 1994 (unpublished).

[27] E. S. Phinney, Astrophys. J. **380**, L17 (1991).

[28] R. Narayan, T. Piran, and A. Shemi, Astrophys. J. **379**, L17 (1991).

[29] M. Bailes, in *Proceedings of I. A. U. Symposium 165, Compact Stars in Binaries*, edited by J. van Paradijs, E. van den Heuvel, and E. Kuulkers (Kluwer Academic Publishers, 1995, in press).

[30] A. V. Tutukov and L. R. Yungelson, Mon. Not. R. Astron. Soc. **260**, 675 (1993).

[31] H. Yamaoka, T. Shigeyama, and K. Nomoto, Astron. Astrophys. **267**, 433 (1993).

[32] V. M. Lipunov, K. A. Postnov, and M. E. Prokhorov, Astrophys. J. **423**, L121 (1994), and related, unpublished work.

[33] C. Kochanek, Astrophys. J. **398**, 234 (1992).

[34] L. Bildsten and C. Cutler, Astrophys. J. **400**, 175 (1992).

[35] G. Quinlan and S. L. Shapiro, Astrophys. J. **321**, 199 (1987).

[36] B. F. Schutz, Nature **323**, 310 (1986).

[37] B. F. Schutz, Class. Quant. Grav. **6**, 1761 (1989).

[38] C. Cutler, T. A. Apostolatos, L. Bildsten, L. S. Finn, E. E. Flanagan, D. Kennefick, D. M. Markovic, A. Ori, E. Poisson, G. J. Sussman, and K. S. Thorne, Phys. Rev. Lett. **70**, 1984 (1993).

[39] T. A. Apostolatos, C. Cutler, G. J. Sussman, and K. S. Thorne, Phys. Rev. D **49**, 6274 (1994).

[40] C. W. Lincoln and C. M. Will, Phys. Rev. D **42**, 1123 (1990).

[41] L. E. Kidder, C. M. Will, and A. G. Wiseman, Phys. Rev. D **47**, 3281 (1993).

[42] C. M. Will, in *Relativistic Cosmology*, edited by M. Sasaki (Universal Academy Press, 1994), p. 83.

[43] L. E. Kidder, Phys. Rev. D (1995, in press).

[44] C. Cutler and E. E. Flanagan, Phys. Rev. D **49**, 2658 (1994).

[45] L. S. Finn and D. F. Chernoff, Phys. Rev. D **47**, 2198 (1993).

[46] E. Poisson and C. M. Will, Phys. Rev. D (1995, submitted).

[47] P. Jaranowski and A. Krolak, Phys. Rev. D **49**, 1723 (1994).

[48] L. Blanchet, T. Damour, B. R. Iyer, C. M. Will, and A. G. Wiseman, Phys. Rev. Lett. (1995, submitted).

[49] E. Poisson and M. Sasaki, Phys. Rev. D (1995, in press).

[50] M. Shibata, M. Sasaki, H. Tagoshi, and T. Tanaka, Phys. Rev. D (1995, in press).

[51] H. Tagoshi and T. Nakamura, Phys. Rev. D **49**, 4016 (1994).

[52] H. Tagoshi and M. Sasaki, Prog. Theor. Phys. **92**, 745 (1994).

[53] C. Cutler and E. E. Flanagan, Phys. Rev. D, paper in preparation.

[54] A. Ashtekar, in *Gravitational Radiation*, edited by N. Deruelle and T. Piran, (North Holland, Amsterdam, 1983), p. 421.

[55] B. S. Sathyaprakash, Phys. Rev. D **50**, R7111–R7115 (1994).

[56] A. Królak, K. D. Kokkotas, and G. Schäfer, in *Proceedings of the 17th Texas Symposium on Relativistic Astrophysics*, Ann. N. Y. Acad. Sci. (1995, in press).

[57] T. A. Apostolatos, Phys. Rev. D (1995, in press).

[58] T. Damour and K. Nordtvedt, Phys. Rev. D **48**, 3436 (1993).

[59] C. M. Will, Phys. Rev. D **50**, 6058 (1994).

[60] D. Markovic, Phys. Rev. D **48**, 4738 (1993).

[61] D. F. Chernoff and L. S. Finn, Astrophys. J. Lett. **411**, L5 (1993).

[62] F. D. Ryan, L. S. Finn, and K. S. Thorne, Phys. Rev. Lett. (1995, in preparation).

[63] E. E. Flanagan and S. A. Hughes, Phys. Rev. D (1995, in preparation).

[64] Numerical Relativity Grand Challenge Alliance, 1995. References and information on the World Wide Web, http://jean-luc.ncsa.uiuc.edu/GC/.

[65] B. J. Meers, Phys. Rev. D **38**, 2317 (1988).

[66] D. Kennefick, D. Laurence, and K. S. Thorne, Phys. Rev. D (in preparation).

[67] M. Shibata, T. Nakamura, and K. Oohara, Prog. Theor. Phys. **89**, 809 (1993).

[68] F. A. Rasio and S. L. Shapiro, Astrophys. J. **401**, 226 (1992).

[69] T. Nakamura, in *Relativistic Cosmology*, edited by M. Sasaki (Universal Academy Press, 1994), p. 155.

[70] X. Zhuge, J. M. Centrella, and S. L. W. McMillan, Phys. Rev. D **50**, 6247 (1994).

[71] M. B. Davies, W. Benz, T. Piran, and F. K. Thielemann, Astrophys. J. **431**, 742 (1994).

[72] D. Christodoulou, Phys. Rev. Lett. **67**, 1486 (1991).

[73] K. S. Thorne, Phys. Rev. D **45**, 520–524 (1992).

[74] A. G. Wiseman and C. M. Will, Phys. Rev. D **44**, R2945 (1991).

[75] D. Kennefick, Phys. Rev. D **50**, 3587 (1994).

[76] A. G. Petschek, *Supernovae* (Springer Verlag, 1990).

[77] H. A. Bethe, Rev. Mod. Phys **62**, 801 (1990).

[78] A. Burrows, J. Hayes, and B. A. Fryxell, Astrophys. J. (1995, in press).

[79] A. Burrows (1995, private communication).

[80] L. S. Finn, Ann. N. Y. Acad. Sci. **631**, 156 (1991).

[81] R. Mönchmeyer, G. Schäfer, E. Müller, and R. E. Kates, Astron. Astrophys. **256**, 417 (1991).

[82] D. Lai and S. L. Shapiro, Astrophys. J. **442**, 259 (1995).

[83] J. L. Houser, J. M. Centrella, and S. C. Smith, Phys. Rev. Lett. **72**, 1314 (1994).

[84] I. A. Bonnell and J. E. Pringle, Mon. Not. R. Astron. Soc. **273**, L12 (1995).

[85] M. Zimmermann and E. Szedenits, Phys. Rev. D **20**, 351 (1979).

[86] S. L. Shapiro and S. A. Teukolsky, Wiley: Interscience, 1983. Section 10.10 and references cited therein.

[87] B. F. Schutz (1995, private communication).

[88] S. Chandrasekhar, Phys. Rev. Lett. **24**, 611 (1970).

[89] J. L. Friedman and B. F. Schutz, Astrophys. J. **222**, 281 (1978).

[90] R. V. Wagoner, Astrophys. J. **278**, 345 (1984).

[91] L. Lindblom, Astrophys. J. **438**, 265 (1995).

[92] L. Lindblom and G. Mendell, Astrophys. J. **444**, 804 (1995).

[93] J. Armstrong, P. Bender, D. Eardley, C. W. F. Everitt, R. Hellings, K. Nordtvedt, H. J. Paik, R. Reasenbert, I. Shapiro (chair), J. Taylor, K. Thorne, R. Weiss, and C. Will, *Report of the Ad Hoc Committee on Gravitation Physics and Astronomy,* Astrophysics Division, NASA Headquarters (Washington, DC, 1990).

[94] P. Bender, A. Brillet, I. Ciufolini, K. Danzmann, R. Hellings, J. Hough, A. Lobo, M. Sandford, B. Schutz, and P. Touboul, *LISA, Laser Interferometer Space Antenna for Gravitational Wave Measurements: ESA Assessment Study Report.* R. Reinhard, ESTEC, 1994.

[95] D. Hils, P. Bender, and R. F. Webbink, Astrophys. J. **360**, 75 (1990).

[96] L. S. Finn and K. S. Thorne, Phys. Rev. D (1995, in preparation).

[97] F. D. Ryan, Phys. Rev. D (1995, in preparation).

[98] D. Molteni, G. Gerardi, and S. K. Chakrabarti, Astrophys. J. **436**, 249 (1994).

[99] D. Hils and P. Bender (1995, preprint).

[100] Y. B. Zel'dovich and I. D. Novikov, *Relativistic Astrophysics Volume 2, The Structure and Evolution of the Universe* (University of Chicago Press, 1983), pp. 160–163.

[101] L. P. Grishchuk, Soviet Physics–JETP **40**, 409 (1974).

[102] L. P. Grishchuk, Class. Quant. Grav. **10**, 2449–2477 (1993).

[103] E. E. Flanagan, Phys. Rev. D **48**, 2389 (1993).

[104] E. Witten, Phys. Rev. D **30**, 272 (1984).

[105] A. Kosowsky and M. S. Turner, Phys. Rev. D **49**, 2837 (1994).

[106] A. Vilenkin, in *Three Hundred Years of Gravitation*, edited by S. W. Hawking and W. Israel (Cambridge University Press, 1987), pp. 499–523.

[107] T. Vachaspati and A. Vilenkin, Phys. Rev. D **31**, 3052 (1985).

[108] G. E. Moss, L. R. Miller, and R. L. Forward, Applied Optics **10**, 2495 (1971).

[109] K. S. Thorne, in *Relativistic Cosmology*, edited by M. Sasaki (Universal Academy Press, 1994), p. 67.